Earthquake (2025) Volume 3 Issue 2 ISSN: 3029-1550 (O)
doi: 10.59429/ear.v3i2.8890

RESEARCH ARTICLE

Roanoke River lineament and other geomorphic anomalies in the Coastal Plain of northeastern North Carolina, USA: LiDAR evidence for late Quaternary tectonics

Ronald T. Marple[1,*], James D. Hurd, Jr.[2]

[1] *302 Riverplace West, Gatesville, TX 76528, USA*

[2] *Department of Natural Resources and the Environment, The University of Connecticut U-87, Room 308, 1376 Storrs Road, Storrs, CT 06269-4087, USA*

*** Corresponding author:** Ronald T. Marple, ronmarple@verizon.net

ABSTRACT

LiDAR images of northeastern North Carolina in the southeastern USA revealed a ~60-km-long, E-W-oriented geomorphic lineament that crosses the northern side of the Albemarle embayment, herein named the Roanoke River lineament. It is defined by morphological changes along the Roanoke River valley northeast of Palmyra that are aligned with a gentle ~40-km-long, E-W-oriented, south-facing topographic scarp to the east and an angular stream bend to the west. Based on its oblique orientation relative to the regional ENE-WSW-oriented horizontal compressive stress field, S_{Hmax}, and the style of geomorphic anomalies that define the lineament, we interpret the Roanoke River lineament to be the surface expression of a buried sinistral strike-slip fault zone, named herein the Roanoke River fault zone. This proposed fault zone may have formed to accommodate the dilatational change in volume produced by dextral motion across the ~10-km-wide Tar River right-step releasing offset in the dextral East Coast strike-slip fault system (ECFS) beneath the Atlantic Coastal Plain of the southeastern USA. North of the Roanoke River lineament is the ~55-km-long, WNW-ESE-oriented Corduroy Swamp lineament that coincides with the western Norfolk arch. Based on its oblique orientation relative to S_{Hmax} and the geomorphic evidence for uplift along the lineament, we postulate that it is the surface expression of a buried transpressional sinistral strike-slip fault, herein named the Corduroy Swamp fault. The existence of these and other faults interpreted herein could have major implications for the tectonic development of the Albemarle embayment and Norfolk arch along the Atlantic continental margin.

Keywords: Roanoke River lineament; Roanoke River fault zone; East Coast fault system (ECFS); Tar River right-step releasing offset (TRO); Corduroy Swamp lineament; Corduroy Swamp fault; Tarboro fault zone; transtension

1. Introduction

The study area coincides with the Albemarle embayment and Norfolk arch in the Coastal Plain of northeastern North Carolina in the southeastern USA where little seismicity has been recorded and few buried, potentially active faults have been identified (**Figure 1**). Despite the low-level seismicity and thick Coastal Plain sediments in the study area, long-term deformation of the Coastal Plain sediments above a buried active

ARTICLE INFO
Received: 17 February 2025|Accepted: 1 July 2025|Available online:23 July 2025

CITATION
R. T. Marple, J. D. Hurd, Jr. Roanoke River lineament and other geomorphic anomalies in the Coastal Plain of northeastern North Carolina, USA: LiDAR evidence for late Quaternary tectonics. *Earthquake*. 2025; 3(2): 8890.doi: 10.59429/ear.v3i2.8890

fault zone can produce subtle geomorphic anomalies that LiDAR (Light Detection and Ranging) data can detect. The goal of this study was therefore to find evidence of potentially active faults beneath the Coastal Plain of northeastern North Carolina using primarily LiDAR data. Our results suggest that potentially active faults are hidden beneath this area.

One of the largest known buried faults beneath the North Carolina Coastal Plain is the ~80-km-long, NE-SW-oriented Graingers fault or wrench zone (GFZ) along the northwestern edge of the Precambrian to Paleozoic Graingers basin or synform in the pre-Cretaceous basement (Brown *et al.* 1977, 1982; Daniels and Zietz 1978) (**Figure 1**). This buried sinistral en echelon wrench fault zone bounds a series of NE-plunging grabens, half-grabens, and a central horst beneath the Coastal Plain. Just west of the NE-SW-oriented segment of the Neuse River near Kinston is the ~10-km-long, NE-SW-oriented, SE-facing Jericho Run fault line scarp (**Figure 1**) that has undergone Paleocene to Holocene deformation (Brown *et al.* 1977; McLaurin and Harris 2001). Approximately 25 km south-southeast of this scarp is a small, ~9-km-long, ~1.5-m-high, NNE-SSW-oriented, east-facing scarp that crosses the southern end of the buried Graingers basin (Carter and McLaurin 2019, fig. 5). Small historical earthquakes near the southern end of the GFZ (**Figure 1**) (Kohler 1976; United States (U.S.) Geological Survey 2022) suggest that deformation is ongoing along the GFZ.

Carter and McLaurin (2019) examined 64 km of riverbank exposures along the Tar and Neuse rivers west of the GFZ to search for seismically induced paleoliquefaction deposits in the presently aseismic inner Coastal Plain of east-central North Carolina. They determined that most of these exposures are Cretaceous to Paleogene sediments that are too old and compacted to liquefy during an earthquake. Because they found no evidence for paleoliquefaction along these two rivers, they concluded that no large Holocene earthquakes have occurred along the inner Coastal Plain of east-central North Carolina.

Using shallow (9-34 m deep), coarsely spaced (>10 km) core-hole data from Weems and Lewis (2007), Weems *et al*. (2009) interpreted six steeply dipping buried faults beneath the inner Coastal Plain of northeastern North Carolina─the Thornburg, Fountains Creek, Stony Creek, City Point, Palmyra, and Whitakers faults (**Figure 2a**). They hypothesized that these faults were active during the Cretaceous and, except for the Fountains Creek fault, underwent further minor displacements during the Cenozoic. No lineaments or other geomorphic anomalies were detected along these interpreted faults on the LiDAR images examined herein.

Based mainly on shallow core-hole data, the right-lateral deflection of the Neuse River near Smithfield, and the deep incision of the Cape Fear River and upwarped Pleistocene fluvial terraces northeast of Fayetteville, Brown *et al.* (1979), Soller (1983, 1988), and Markewich (1985) postulated that a ~100-km-long, NE-SW-oriented fault or flexure crosses the inner Coastal Plain of southeastern North Carolina. Soller (1988) concluded that uplift began along this trend ~750 ka and that it reached its maximum uplift rate during the past 70 ka. Marple (1994) later postulated that these geomorphic anomalies are associated with a larger buried dextral strike-slip fault system beneath the Coastal Plain of the Carolinas. Marple and Talwani (2000) postulated that this fault system continues northeastward into southeastern Virginia and named it the East Coast fault system (ECFS). They interpreted two ~10-km-wide right-step offsets along the ECFS─one in northeastern South Carolina and the other in east-central North Carolina, referred to herein as the Tar River releasing offset (TRO) (**Figure 1**). Marple and Hurd (2021) reinterpreted the location of the ECFS near Fayetteville, which resulted in its alignment with the southern ECFS (ECFS-S) in northeastern South Carolina where it forms the interpreted ~17º Cape Fear restraining fault bend (**Figure 1**). The northeastern end of the ECFS-S in east-central North Carolina coincides with an area of surface faults near the Fall Line that offset Pliocene-Pleistocene strata (Prowell 1983) (**Figure 1**).

2. Methodology

2.1 The use of LiDAR data to detect buried active faults beneath the U.S. Atlantic Coastal Plain

The LiDAR data used in this study were acquired as part of the Floodplain Mapping Program (NCFMP) in 2014 and 2015 by Quantum Spatial, Inc. (National Oceanic and Atmospheric Administration (NOAA) Office for Coastal Management 2015). Point data were collected at a nominal pulse spacing of 0.7-1.5 m. Project specifications were based on the U.S. Geological Survey National Geospatial Program LiDAR Base Specification, version 1. These data were created using the horizontal projection/datum of the North Carolina State Plane Coordinate System, NAD 83, and vertical datum NAVD 88 (GEOID12A). The LiDAR data, initially in RAW flight line swath format, were downloaded by county from the NOAA Office for Coastal Management (2015) and then converted to Classified LAS 1.4 files. We reformatted the LAS files to 5000-ft (~1500 m) tiles to generate bare earth digital elevation models (DEMs) at a 5-ft (~1.5 m) spatial resolution. We then mosaicked these DEM tiles into individual areas of interest.

We used the Hillshade tool in ArcGIS to generate shaded relief images with various illumination azimuths, an elevation angle of 25°, and a vertical exaggeration of 10-15X. A major advantage of these processing parameters is that they enhance subtle, tectonically deformed landforms in intraplate settings that would otherwise be difficult to detect using conventional aerial photographs, satellite images, and topographic maps (Marple and Hurd 2020, 2021, 2022). We then generated color relief images using a color scheme based on terrain elevations, followed by contrast adjustments in Adobe Photoshop. We further improved low contrast images using the intensity-hue-saturation (IHS) routine. The LiDAR data were also used to construct detailed topographic profiles to quantify elevation changes across landforms that we suspected were tectonically deformed, similar to the way in which topographic profiles in other intraplate areas have been used globally to analyze fault scarps, uplifted fluvial terraces, and other deformed landforms indicative of active tectonics (e.g., Nazari *et al.* 2014; Peri *et al*. 2022; Kaveh-Firouz *et al.* 2024; Oliva *et al.* 2024).

2.2 The use of river morphology to detect buried active faults beneath the U.S. Atlantic Coastal Plain

Compressional deformation has been dominant along faults in the eastern USA during the Cenozoic (e.g., Prowell 1988). Such deformation along buried active faults beneath the Atlantic Coastal Plain produces a zone of gentle uplift several kilometers wide within the overlying sediments. This uplift causes anomalous changes in river geomorphology above buried active faults called river anomalies. The uplift changes the slope of meandering alluvial rivers, which changes their stream power locally (i.e., product of stream discharge and channel slope, Schumm *et al*. 2000). Valley-floor steepening immediately downstream from the uplift axis increases stream power, which causes the channel to incise across the uplift axis and produce knickpoints (sharp changes in channel bed slope) that migrate upstream (Ouchi 1985). The river along the steepened reach tries to maintain equilibrium by increasing its sinuosity downstream. The increased sinuosity decreases the sediment-carrying capacity of the channel, which causes aggradation (deposition) downstream. The decreased valley slope and sediment-carrying capacity upstream from the uplift axis also cause channel aggradation. Continued aggradation upstream can cause flooding and the development of anastomosing stream patterns upstream. Sustained uplift upwarps floodplains and terraces.

The most impressive example of uplift-induced river incision and upwarped fluvial terraces in the U.S. Atlantic Coastal Plain occurs along the Cape Fear River valley between Fayetteville and Dunn, North Carolina. Here, late Quaternary uplift along this part of the ECFS-S has caused the Cape Fear River to incise up to 18 m through the Coastal Plain sediments and underlying Cretaceous formations (**Figure 3**, Marple and Hurd 2021,

figs. 8 and 17, profile 12). Rapid uplift can also interrupt small drainages, such as that along the E-W-oriented Mount Holly lineament (MHL) in the meizoseismal area of the 1886 Charleston, South Carolina, earthquake in the outer Coastal Plain of the southeastern USA (Marple and Hurd 2020, fig. 5, profile 22). Marple and Hurd (2020) postulated that uplift along a buried active fault associated with the MHL was rapid enough to interrupt the once continuous drainage along the N-S-oriented Sophia and Brick Bound swamps.

Angular stream bends, linear topographic depressions and stream segments, and rectangular or rectilinear topographic depressions have also been used to identify buried, potentially active faults beneath the U.S. Atlantic Coastal Plain (Marple and Hurd 2020, 2021, 2022). One of the most dramatic examples of a rectangular topographic depression in the Coastal Plain sediments is the Foster Creek depression (FCD) at the eastern end of the ~40-km-long, E-W-oriented Deer Park lineament (DPL) in the meizoseismal area of the 1886 Charleston, South Carolina, earthquake (Marple and Hurd 2020, figs. 3 and 6a). This unusual 3-sided depression is ~2 × 2.5 km in size, ~7- to 8-m-deep, and bounded by relatively steep scarps intersecting at ~90°. Marple and Hurd (2020) attributed the FCD to subaerial erosion along a buried active fault zone associated with the DPL, which they hypothesized may have ruptured during the 1886 Charleston earthquake. Southwest of the DPL are examples of linear topographic depressions in the Coastal Plain sediments at the western end of the ENE-WSW-oriented Middleton Place fault zone (MPF) (Marple and Hurd 2020, fig. 7). Marple and Hurd (2020) attributed these linear depressions to subaerial erosion along the MPF. These and other types of tectonically deformed landforms are summarized in Howard (1967), Glass and Slemmons (1978), Schumm *et al.* (2000), and Marple and Hurd (2020, 2021, 2022). We sought these and other types of geomorphic anomalies to identify buried active faults beneath the Coastal Plain of northeastern North Carolina.

We calculated channel sinuosities along the Roanoke River to quantify changes in its sinuosity across the Roanoke River lineament (RRL). Channel sinuosity was calculated as channel length divided by the shortest distance along this part of the channel (Schumm *et al*. 2000). Because of the large variations in sinuosity along the river (**Figure 4a**), we divided the river valley into three segments to calculate the sinuosities─the river valley between the entrenched meander at Halifax (**Figure 2a**) and the large river deflection near Palmyra, the valley downstream from the large river deflection where the valley displays a down-to-the-southwest cross-valley tilt, and the valley farther downstream between Hamilton and the Albemarle Sound. We then subdivided these three parts of the river valley into smaller segments that were twice the average meander wavelength of each of the three valley segments. The average meander wavelengths were ~3 km for the valley upstream from the river deflection, ~2 km along the part of the valley that displays a down-to-the-southwest cross-valley tilt, and ~11 km for the valley downstream from Hamilton.

We examined surficial geologic maps of northeastern North Carolina (Brown *et al*. 1985; Weems *et al*. 2009) and constructed elevation profiles across the Roanoke River valley using the LiDAR data to evaluate evidence for and against late Quaternary deformation along the RRL and the Corduroy Swamp lineament (CSL). We also used the LiDAR data to search for possible geomorphic evidence of paleoliquefaction from Holocene earthquakes. Lastly, we further examined selected geomorphic features suspected of being tectonically deformed landforms in the field.

3. Geologic and geomorphic setting of the Albemarle embayment

3.1 Terraces and paleo-littoral scarps

Gentle ongoing subsidence of the U.S. Atlantic Coastal Plain and transgressive-regressive cycles caused by glacioeustatic sea level fluctuations across the Albemarle embayment and Norfolk arch during the Cenozoic era (Cronin 1981) resulted in a series of emergent marine terraces in the southeastern USA. These terraces are

best preserved and youngest toward the coast. Terrace landforms include estuarine plains, back-barrier marshes, lagoonal deposits, and sandy barrier island ridges (Colquhoun *et al*. 1991; Soller and Mills 1991). The terraces are bounded on their seaward (east) side by eroded paleo-littoral scarps, such as the early Pleistocene Surry and late Pleistocene Suffolk scarps (Cronin *et al.* 1984; Ator *et al*. 2005) (**Figure 4**). Sandy beach ridge deposits bound the western side of these paleoshoreline scarps.

3.2 Carolina bays and pocosins

A common landform in the North Carolina Coastal Plain are Carolina bays. Carolina bays are shallow, NW-SE-oriented, elliptical-shaped depressions of varying sizes that are often occupied by ponds and wetlands. They commonly have elevated rims composed of fine sand to gravel that were deposited by high-energy, lacustrine shoreface and eolian processes (Soller 1988; Moore *et al*. 2016). Carolina bays formed by winds shifting from northwest to southwest between 100 and 200 ka (Soller and Mills 1991). They are therefore absent on Holocene floodplains and late Pleistocene terraces younger than 100 ka.

There are also low-lying ovoid to irregularly shaped topographic depressions known as pocosins (Richardson 1981) in the North Carolina Coastal Plain, which range in size from tens of meters to several kilometers. The circular to irregular shapes of pocosins, combined with their lack of elevated sand rims, help to distinguish them from Carolina bays. Pocosins contain peaty material that accumulated over thousands of years during Holocene time when water tables were high and oxidation low (Richardson 1981). Forest fires during Quaternary droughts burned away some of the dried peat deposits. Shallow water tables during wetter times allowed the peat and muck to accumulate again. The organic matter in pocosins caused the soil to be highly acidic and nutrient deficient. Weems *et al.* (2009) postulated that many of the smaller pocosins may have formed within the topographic depressions of Holocene seismically induced sandblows. LiDAR images examined herein revealed that some pocosins may have also formed in Carolina bays, such as the large Roquist pocosin that is developed in sedimentary unit Qch (**Figure 2a**). The Roquist pocosin, like Carolina bays, is elliptical, has raised rims along its southeastern border, and is oriented NW-SE.

3.3 Fluvial geomorphology

The predominant drainage pattern in the North Carolina Coastal Plain is dendritic (e.g., Marple and Hurd 2021, fig. 11) (**Figures 4** and **5**). Superimposed on this drainage pattern are angular stream bends that are likely associated with Quaternary joints or faults in the near-surface sediments (e.g., Marple and Hurd 2020, 2021). The most impressive example of an angular stream bend in the Atlantic Coastal Plain is the barbed bend along Livingston Creek that partly defines the Livingston Creek lineament in southeastern North Carolina (Marple and Hurd 2021, fig. 11). Some Coastal Plain rivers have also been deflected to the south-southwest by bay-mouth shifting caused by longshore drift to the south-southwest along Pliocene-Pleistocene shorelines (e.g., Gayes *et al*. 1992). For example, the Chowan River in northeastern North Carolina is deflected ~30 km southward around the beach ridge deposit along the western side of the Suffolk scarp (**Figure 4**).

3.4 Floodplain and terrace sediments of the Roanoke and Tar river valleys

The alluvial sediments of the Roanoke River valley in the North Carolina Coastal Plain range in age from middle Pleistocene to Holocene (Weems *et al*. 2009). The sediments beneath the oldest alluvial terrace, unit Qch, consist of middle Pleistocene (450-400 ka) silty and clayey sand of the Chuckatuck Formation (**Figure 2a**). Late Pleistocene (20-10 ka), medium- to coarse-grained silty sand containing gravel and quartz pebbles (**Figure 2a**, unit Qalb) underlies the next younger alluvial terrace. This terrace is absent south of the Roanoke River's deflection northeast of Palmyra (**Figure 2a**). Upstream from this river deflection, the channel flows over sediments of the late Cretaceous Cape Fear (Kcf) and Clubhouse (Kcl) formations (Brown *et al.* 1985). These Cretaceous sediments are also exposed locally along bluffs near the river upstream from Palmyra

(**Figure 2a**). The modern floodplain (**Figure 2a**, unit Qal) consists of fine- to coarse-grained sand containing quartz pebbles (Weems *et al*. 2009).

The Tar River valley southeast of Tarboro is underlain by a modern floodplain and unpaired Pleistocene alluvial terraces to the east and northeast (Moore and Daniel 2011) (**Figure 1**). These terraces consist of late Pleistocene lower and upper paleo-braidplains and the Upland alluvial terrace. The paleo-braidplains are underlain by fine- to coarse-grained sand containing pebbles and minor amounts of cobbles and boulders that were deposited during the late Pleistocene when the Tar River was braided (Moore and Daniel 2011). The paleo-braidplains are locally overlain by late Pleistocene eolian sand dunes that have U-shaped parabolic, transverse, and irregular morphologies (Moore and Daniel 2011). Above the upper paleo-braidplain is the Upland alluvial terrace, which is at least 100 ka in age based on the presence of Carolina bays. These unpaired terraces indicate that the river southeast of Tarboro has mysteriously migrated ~13 km to the west-southwest during late Pleistocene-Holocene time. O'Driscoll *et al*. (2010) postulated that the unpaired terraces could be from Quaternary tectonic uplift to the northeast. We later present an alternative explanation for this cross-valley tilt based on transtension along a curve in a buried sinistral strike-slip fault.

3.5 Subsurface sediments and bedrock geology

Fluvial processes and glacioeustatic sea level fluctuations in the Coastal Plain of northeastern North Carolina since the early Cretaceous have resulted in a coastward-thickening wedge of southeast-dipping, Cretaceous and younger sediments and sedimentary rocks beneath the Coastal Plain that thicken to ~3 km near the coast (Gohn 1988; Weems *et al*. 2019). The Cretaceous formations in northeastern North Carolina include the Lower Cretaceous Patuxent Formation and the Upper Cretaceous Donoho Creek, Caddin, Shephard Grove, Pleasant Creek, Cape Fear, and Clubhouse formations (Weems *et al*. 2009). These Cretaceous formations consist primarily of marine siliciclastic sediments (Gohn 1988).

The Cretaceous formations unconformably overlie an eastward-dipping crystalline basement composed of igneous and metamorphic rocks of the Roanoke Rapids terrane and Hatteras belt near the coast. The unconformity at the base of the Cretaceous formations is the time-transgressive postrift unconformity (PRU) that separates the eroded prerift and syn-rift rocks from the overlying postrift strata along the Atlantic margin (Withjack *et al.* 2020). The Roanoke Rapids terrane consists of slaty to schistose metamorphosed mafic, intermediate, and felsic tuffs and flows, volcaniclastic mudstones, siltstones, and sandstones (Lawrence and Hoffman 1993). The Hatteras belt to the east consists of granitic batholiths, which are bordered to the west by amphibolite facies rocks (Horton *et al*. 1989). Cutting through the Hatteras belt is the NE-SW-oriented, ~20-km-wide Precambrian to Paleozoic Graingers basin or synform (Daniels and Zietz 1978) (**Figure 1**). This basin contains up to 7,000 ft (~2100 m) of low-gradient greenschist facies phyllite (Sampair 1979).

Weems *et al.* (2009) identified Triassic red beds in the bottom of a deep drill-hole north of the lower Roanoke River valley (**Figure 2a**, well RE-4-02). However, no other subsurface data shows evidence of Triassic sediments beneath this part of the North Carolina Coastal Plain (e.g., Lawrence and Hoffman 1993). Thus, any Mesozoic basin associated with these red beds would be too small to be resolved with seismic-reflection, drill-hole, and potential field data.

3.6 Tar kilns

Tar kilns are anthropogenic landforms in the Coastal Plain and Sand Hills region and along the Gulf Coast province of the southeastern USA. These features are typically expressed as small ring-shaped mounds of soil with a central depression and a surrounding shallow trench (Harrup 2013; Snitker *et al*. 2022) (**Figures 6a** and **6b**). Tar kilns are commonly 6 to 22 m in diameter and <1 m high although they can be up to 2 m high. Tar kilns can also be flat topped, have multiple inner rings, or lack a soil mound, sometimes leaving only a

depression in the ground surface where a barrel was placed to collect the tar (**Figures 6b-6e**). Tar kilns occur in areas of high ground as well as in low lying areas where long leaf pine forests were once common. They were created during the early history of the U.S. by piling up long leaf pine logs on a clay floor. The logs were then covered with soil and set afire to smolder. The heat cooked the sap out of the logs, which then drained into a barrel that was placed in a 3- to 4-ft-wide, 1- to 2-ft-deep depression that was commonly dug near the edge of the kiln. These depressions are preserved along the edges of some tar kilns today (**Figures 6b** and **6e**). As the logs burned to ash, the central part of the mound typically collapsed to form an elevated ring of soil. Thus, charred wood is common beneath the soil of tar kilns. The tar was used to waterproof wooden ships of the time (Harrup 2013).

4. Roanoke River lineament (RRL) and other geomorphic anomalies possibly associated with the RRL

4.1 Roanoke River lineament (RRL)

The ~60-km-long, E-W-oriented Roanoke River lineament (RRL) is defined by numerous geomorphic anomalies that cross various Coastal Plain sediments of northeastern North Carolina. The most conspicuous of these anomalies are the abrupt ~8-km-wide southwest deflection of the Roanoke River northeast of Palmyra, a ~45-km-long, 3- to 7-m-high, E-W-oriented, south-facing monoclinal-like scarp to the east between the Roanoke and Chowan rivers, and a right-angle bend along a Deep Creek tributary ~4 km west of Palmyra (**Figures 5** and **7**). The bend in the tributary trends ~20º more to the northeast than the scarp along the eastern RRL, indicating that the western RRL bends ~20º toward the southwest near Palmyra. The scarp along the eastern RRL is formed in early Pleistocene sediments of the Charles City Formation (**Figure 2a**, unit Qcc) whereas the angular bend in the Deep Creek tributary is developed in early Pleistocene sediments of the Windsor Formation (**Figure 2a**, unit Qw). Small streams north of the scarp form a small drainage divide (**Figure 5**), which is consistent with uplift north of the scarp (Marple and Hurd 2021). Another observation that could be from uplift north of the eastern RRL is the alignment of the N-S-oriented Wildcat and Whiteoak swamps across the western end of the drainage divide near Askewville, North Carolina (**Figure 5**), which suggests that they could have once formed a continuous drainage before they were interrupted by uplift north of the scarp.

The Roanoke River's meandering pattern also changes dramatically across the RRL. The river upstream from the RRL meanders freely across a 1- to 3-km-wide floodplain (**Figure 2a**, unit Qal) that narrows to ~1 km just upstream from the RRL. Downstream, the Holocene valley widens dramatically to at least 8 km where it displays a gentle down-to-the-southwest cross-valley tilt. Here, the river is actively eroding the middle Pliocene sediments of the Rushmere and Morgerts Beach members (unit Tyrm) of the Yorktown Formation (Weems *et al*. 2009) along its southwestern valley wall (**Figures 2a** and **8a**, profile 5).

The terrace patterns along the Roanoke River valley also change across the RRL. First, the middle Pleistocene terrace underlain by unit Qch occurs on both sides of the river valley upstream from the RRL (**Figure 2a**). Downstream, it occurs only along the northeastern side of the river valley. Second, the late Pleistocene terrace underlain by unit Qalb upstream from the RRL is absent to the south (**Figure 2a**). Third, the modern floodplain upstream from the RRL is entrenched 2-7 m below the terrace underlain by unit Qalb. The channel upstream from the RRL is also 4 to 6 m deeper than that downstream (**Figure 8a**, profiles 1-5). Lastly, the modern floodplain (unit Qal) just upstream from the RRL is entrenched ~2 m below a low terrace that is associated with older Holocene alluvial sediments labeled Qal2 in **Figures 2a** and **8a** (profile 5).

The sinuosity of the Roanoke River also changes across the RRL. Its sinuosity upstream from the RRL is moderately high where it meanders freely across its modern floodplain (**Figure 9**). It then decreases sharply downstream where the river flows against its southwestern valley wall. It then dramatically increases downstream from Hamilton where the river again meanders freely across a broad, 8- to 10-km-wide floodplain before emptying into Albemarle Sound (**Figures 4** and **9**). Except for the large, late Pleistocene meander loop at Halifax (**Figure 2a**), which became entrenched ~6 m below the terrace associated with surficial unit Qalb during the Holocene, the meander loops upstream from the RRL are much smaller than those downstream from Hamilton (**Figure 4**). Numerous smaller meanders are also superimposed on the large meanders downstream between Hamilton and Jamesville (**Figure 4**), which suggests that there may have been two separate large inputs of sediment into this part of the river.

4.2 Other right-angle stream bends and rectangular topographic depressions along the inner Coastal Plain of northeastern North Carolina

Several NE-SW-oriented, right-angle stream bends occur west of the Roanoke River valley along Deep Creek, Fishing Creek, and the Tar River, most of which parallel the bend in the Deep Creek tributary west of Palmyra (**Figures 7** and **10)**. For example, the Tar River southeast of Tarboro forms a notable ~3.5-km-long right-angle bend to the southwest (**Figure 10**). This river bend is aligned with the northwestern edge of the unpaired terraces along the northeastern side of its lower valley southeast of Tarboro.

Northeast of Tarboro are two right angle bends in Fishing Creek that coincide with two NE-SW-oriented rectilinear topographic depressions in the valley floor (**Figure 10**, sites X and Y). The larger depression near Lawrence (site Y) is ~4 km long, ~1.5 km wide, and ~4-5 m deep, while the smaller depression to the north (site X) is ~3.5 km long, ~1.2 km wide, and ~4-5 m deep. The NE-SW orientations of the rectilinear depressions are oblique to the NNE-SSW-oriented Surry paleo-littoral scarp (**Figure 10**), suggesting that their formation was not influenced by this paleoshoreline. The channel crossing the larger depression near Lawrence is ~5 m deeper than that upstream or downstream. This area of increased incision coincides with sandy beach ridge deposits along the western side of the Surry paleo-littoral scarp.

An IHS-enhanced version of the LiDAR image in **Figure 4a** revealed a ~10-km-wide terrace labeled A south of the monoclinal scarp that defines the eastern RRL (**Figure 4b**, green pattern; **Figure 8b**, profiles 8 and 9). Terrace A is aligned with the area along the Roanoke River valley that displays the down-to-the-SW cross-valley tilt (**Figure 2a**). The southern edge of terrace A is bounded by another, less well developed, E-W-oriented, 5- to 8-m-high topographic scarp that parallels the scarp to the north along the eastern RRL (**Figures 4b** and **8b**, profiles 8 and 9). Terrace A is separated from the terraces of the lower Roanoke River valley to the northwest by an area of high ground that is underlain by early Pleistocene sediments of the Charles City formation (unit Qch, **Figure 2a**).

4.3 Sand mounds, circular topographic depressions, and patches of sand possibly associated with the RRL

4.3.1 Sand mounds along the Roanoke River's natural levees south of the RRL

Downstream from the RRL are over 200, mostly elliptical sand mounds along ~24 km of the Roanoke River's natural levees that are up to 110 m long and 2.5 m high (**Figures 11** and **12**). Most of their long axes are at a high angle to the river (**Figure 12a**). The mounds are composed primarily of medium- to coarse-grained quartz sand that contrasts with the clayey to silty composition of the surrounding floodplain sediments. The mounds are most numerous along the northeastern side of the river (**Figure 11**), opposite the southwestern valley wall where the channel is currently eroding the middle Pliocene sediments of the Rushmere and Morgerts Beach members (unit Tyrm) of the Yorktown Formation (**Figure 2a**). Farther downstream they occur

in smaller groups on either side of the river, commonly appearing on the opposite side of the river near the end of the previous group of mounds (**Figure 11b**). Enlargements of the LiDAR imagery and field reconnaissance revealed that most of the sand mounds have shallow (0.2- to 0.3-m-deep), 1- to 2-m-diameter circular topographic depressions along their crests (**Figure 12a**), sometimes with multiple circular depressions or linear depressions along their axes (e.g., **Figure 12d**). Some depressions along the tops of the mounds are, however, up to 20 m wide (e.g., **Figure 12c**). Numerous 2- to 3-m-wide, shallow (<1 m deep) circular topographic depressions also dot the flanks of some mounds and the surrounding landscape (e.g., **Figure 12d**). The mounds are likely channel deposits that the U.S. Army Corps of Engineers (USACE) dredged from the channel during the 19th and 20th centuries. The origin of the sand mounds is discussed later in the *Discussion* section. Sand from some of the mounds has been excavated to construct nearby dirt roads.

4.3.2 Circular topographic depressions near the RRL

Shallow, 0.8- to 1-m-deep, 80- to 100-m-wide circular topographic depressions occur in an E-W-trending belt mostly north of the RRL (**Figures 5** and **13**). These depressions are developed within the early Pleistocene sediments of the Charles City and Windsor formations, the early Pleistocene Bahramsville unit of the Bacons Castle Formation, and other Coastal Plain sediments (**Figure 2a**). Unlike the elliptical-shaped Carolina bays, these topographic depressions are circular, lack sandy rims, and are slightly raised in the center (**Figure 13b**). The topographic depressions near the RRL are like those on LiDAR images of the meizoseismal area of the 1886 Charleston, South Carolina, earthquake (Marple and Hurd 2020, figs. 4a, 8a, and 14a).

4.3.3 Patches of sand south of the RRL

Light-colored, 5- to 10-m-wide patches of fine quartz sand are common south of the Roanoke River valley (**Figure 14**) where they are formed within the Tertiary Yorktown and Duplin sediments of Brown *et al*. (1985). Similar patches of light-colored sand are common in the New Madrid seismic zone of the northern Mississippi embayment where subsurface investigations and historical records of some of these sands have been confirmed to be seismically induced liquefaction deposits (e.g., Tuttle *et al.* 2019). The similarities in sediment composition and geomorphic settings suggest that the patches of sand south of the Roanoke River valley may also be seismically induced liquefaction deposits.

5. Corduroy Swamp lineament (CSL)

Along the western Norfolk arch of northeastern North Carolina is the ~55-km-long, WNW-ESE-oriented Corduroy Swamp lineament (CSL) (**Figures 1** and **4**). It is defined by a ~12-km-long, WNW-ESE-oriented linear segment of Corduroy Swamp and a ~55-km-long, WNW-ESE-oriented topographically high area (**Figure 4a**, between opposing arrows labeled TH). This topographic high is up to 50 ft (~13.7 m) higher than the terrain to the north and south. This area of high ground is bounded to the north by the Meherrin River and to the south by Potecasi Creek and the Wiccacon River (**Figure 4a**). Late Pliocene-Pleistocene surficial map units Tbv, Qbb, and Qw project eastward along this topographic high. Late Pliocene unit Tbv, for example, turns abruptly eastward ~14 km along this topographic high (**Figure 2a**). The absence of drill-hole data across this topographic high prevents direct measurements of uplift along the CSL, which could be crucial for understanding the style and timing of deformation along the interpreted buried active fault associated with the CSL. The topographically high area along the CSL crosses the northern ECFS (ECFS-N) to the west (**Figure 4a**).

6. Geomorphic anomalies that define the ECFS-N in northeastern North Carolina

The interpretation of the ECFS-N along the inner Coastal Plain of northeastern North Carolina is based mainly on anomalous changes in river morphology. One of the most conspicuous river anomalies along this part of the ECFS-N is the ~16-km-long, NNE-SSW-oriented right-angle stream bend formed by the intersection of the Marsh and Beech swamps (**Figure 2a**). This conspicuous stream bend is anomalous because it is perpendicular to the dominant NW-SE trend of most streams draining the inner Coastal Plain of northeastern North Carolina. The drainage density is also greater along the northwestern side of Marsh Swamp where the swamps are developed within the early Pleistocene Bahramsville unit of the Bacons Castle Formation (**Figure 2a**). The tributary that drains into the southwestern end of Marsh Swamp, Burnt Coat Swamp, is ~2 m higher than Beech Swamp just downstream from (southeast of) Marsh Swamp based on the dry elevated nature of Burnt Coat Swamp compared to the submerged nature of Beech Swamp (**Figure 15**).

Southwest of Marsh Swamp, Fishing Creek and the Tar River are 1-2 m deeper along the ECFS-N (Marple and Talwani 2000). Their valleys also widen abruptly into broad, ~11-km-wide floodplains just downstream from the ECFS-N (**Figure 2a**), which suggests that the area along and west of the ECFS-N has been gently uplifted during the Holocene (Marple and Talwani 2000). Similarly, the Neuse River along the interpreted ECFS-S near Smithfield transitions from a V-shaped valley to a broad floodplain ~3 km downstream from its right-angle bend along the ECFS-S (Marple and Hurd 2021, fig. 3). Another type of geomorphic anomaly that is consistent with local transpressional uplift along the ECFS-N is the local narrowing of the Beaverdam and Burnt Coat swamps and the Fishing Creek valley ("pinched" valleys of Howard 1967) along the western (upstream) side of the ECFS-N (**Figure 2a**).

Southwest of Fishing Creek, Swift Creek's floodplain is a wooded terrace east of the Fall Line where the channel is incised up to 3 m below its floodplain. Eastward, the floodplain gradually transitions into a submerged swamp near the trend of the ECFS-N. Swift Creek's valley is also convex to the north-northeast where it crosses the ECFS-N (**Figure 2a**). Similar convex-shaped river curves occur along the Santee, Black, and Lynches rivers where they cross the ECFS-S in the South Carolina Coastal Plain and along the Nottoway River where it intersects the ECFS-N along the inner Coastal Plain of southeastern Virginia (Marple and Talwani 2000, figs. 5, 7, and 14). Marple and Talwani (2000) postulated that these river curves were produced by a gentle down-to-the-NNE cross-valley tilt along buried, NNE-plunging en echelon fault segments of the ECFS, thus causing these rivers to migrate locally to the north-northeast along the ECFS. We hypothesize that the curve in the Swift Creek valley may have also formed by a down-to-the-NNE cross-valley tilt caused by deformation along buried, NNE-plunging en echelon fault segments beneath this part of the ECFS-N.

Southwest of Swift Creek and along the ECFS-N at Rocky Mount, the Tar River flows over erosionally resistant rocks of the Rocky Mount igneous pluton (gray, white, and pink, fine- to coarse-grained to megacrystic, monzogranite, biotite-rich granite, and granodiorite, age 345±1 Ma, Gay 2004), resulting in several rapids or shoals along this part of the Tar River. The Tar River is also ~3 m deeper where it crosses the ECFS-N.

Several geomorphic anomalies also occur along the Roanoke River valley where it intersects the ECFS-N. First, the valley floor widens abruptly ~7 km downstream from the ECFS-N (**Figure 2a**). Second, the Roanoke River is 4-6 m deeper where it crosses the ECFS-N (**Figure 8**, profiles 1-3). Third, the Roanoke River displays an anastomosing pattern just upstream from the ECFS-N (**Figure 2a**). This fluvial pattern is consistent with gentle back-tilting of the valley floor to the west by uplift along the ECFS-N (Ouchi 1985). Lastly, the

sinuosity increases dramatically downstream from the ECFS-N, as indicated by the large meander near Halifax (**Figure 2a**).

7. Discussion

7.1 Origin of the Roanoke River lineament (RRL)

We evaluated changes in river base level caused by lowering of Pleistocene sea level, lithologic changes in Coastal Plain sediments, joints in the near-surface sediments, and deformation along a buried active fault zone to ascertain the origin of the RRL. The first of these processes, lowering of Pleistocene sea level, cannot explain the geomorphic anomalies along the Roanoke River valley near Palmyra. The nearest paleoshoreline represented by the early Pleistocene Surry scarp crosses the river valley ~18 km upstream from the RRL (**Figure 2a**). Furthermore, although the increased incision along Fishing Creek near Lawrence coincides with the sandy beach ridge deposit along the western side of the Surry scarp, the nearby rectilinear topographic depressions and right-angle stream bends are obliquely oriented to the scarp trend (**Figure 10**). Therefore, it is improbable that these stream bends and rectilinear depressions formed by ancient shoreline processes along the Surry paleoshoreline. Marple and Hurd (2021, fig. 7) noted similar rectangular depressions along the northeastern wall of the South River valley on the Cape Fear arch to the south near Tomahawk, North Carolina. They attributed these rectangular depressions to subaerial erosion along a buried active fault zone. Such angular stream bends and rectilinear depressions are rare in the Atlantic Coastal Plain because the rapid erosion of the unconsolidated, easily eroded Coastal Plain sediments favors dendritic drainage patterns. Thus, angular stream bends and rectangular topographic depressions are not likely to form in the Coastal Plain without the influence of joints or faults in the near-surface sediments (Marple and Hurd 2020, 2021). We, therefore, hypothesize that the rectilinear topographic depressions and angular stream bends near Lawrence were produced by subaerial erosion along joints or faults in the near-surface sediments.

Nor can lithologic changes in the Coastal Plain sediments explain most of the geomorphic anomalies along the RRL. For example, the lithologies of the sediments across the bend in the Deep Creek tributary west of Palmyra (**Figure 7**) do not change across this stream bend (**Figure 2a**). The only geomorphic anomaly that coincides with a lithologic change in the Coastal Plain sediments is the increased incision along Fishing Creek near the sandy beach ridge deposits that coincide with the Surry scarp trend near Lawrence.

Joints in the near-surface sediments also cannot explain all the geomorphic anomalies that define the RRL. For example, the Roanoke River's large deflection northeast of Palmyra and the down-to-the-southwest cross-valley tilt downstream (**Figure 8a**, profiles 5 and 6) suggest that the valley downstream from the RRL has been tilted down-to-the-southwest south of a buried active fault zone associated with the RRL. We suggest that this tilt forced the river downstream from the RRL to migrate laterally to the southwest where it continues to erode its southwestern valley wall (**Figures 5** and **8a**, profile 5). The cross-valley tilt has also prevented this part of the river from developing a freely meandering pattern, like that farther downstream (**Figure 5**).

The Roanoke River's greater incision upstream from the RRL (**Figure 8a**, profiles 1-4), the south-facing scarp along the eastern RRL (**Figure 5**), and the absence of unit Qalb along the Roanoke River valley south of the RRL (**Figure 2a**) are consistent with Holocene, up-to-the-north displacements along a buried, potentially active fault zone, herein named the Roanoke River fault zone (RRFZ) (**Figure 16**). An E-W-oriented drainage divide north of and parallel to the scarp along the eastern RRL (**Figure 5**) supports uplift along the northern side of the eastern RRL. The alignment of the N-S-oriented Wildcat and Whiteoak swamps near the west end of the drainage divide (**Figure 5**) suggests that they could have once formed a continuous drainage that was interrupted by Holocene uplift along the proposed RRFZ. Marple and Hurd (2020) similarly postulated that

uplift along a buried active fault associated with the E-W-oriented Mount Holly lineament (MHL) in the South Carolina Coastal Plain was rapid enough to interrupt the once continuous drainage along the N-S-oriented Sophia and Brick Bound swamps. The gentle slope of the scarp along the eastern RRL and the 200- to 500-m-thick sediments beneath the scarp (Weems *et al.* 2019) suggest that displacements at depth along the interpreted RRFZ have folded rather than displaced the overlying sediments (**Figure 2b**). Faulting beneath thick unconsolidated sediments commonly folds rather than offsets the overlying sediments (Stein and Yeats 1989). If true, the oblique orientation of the interpreted RRFZ relative to S_{Hmax} suggests that the RRFZ is a buried sinistral strike-slip fault zone.

Sinistral displacement along the bend in the western RRFZ near Palmyra (**Figure 16**) favors transtension along this fault bend. We propose that this transtension caused the terrain south of the fault bend to tilt down-to-the-southwest, thereby causing the Roanoke River south of the RRL to migrate laterally to the southwest during Holocene time. The proposed cross-valley tilt could explain why the river's sinuosity downstream from the RRL is unexpectedly lower than that upstream where the river is more deeply incised (**Figure 9**). As stated earlier in the *Methodology* section, local downcutting by a river increases the river's sediment load, thereby causing aggradation and increased sinuosity downstream (e.g., Schumm *et al.* 2000), unless another mechanism prevents the development of meanders downstream from the area of downcutting. We propose that this secondary mechanism is the cross-valley tilt downstream from the RRL, which has prevented this part of the river from developing a meandering pattern, thus causing the unexpectedly low sinuosity downstream from the RRL.

In contrast to the eastern RRL, the angular stream bends to the west (**Figures 7** and **10**) suggest that displacements at depth along the western RRFZ have fractured upward through the thinner sediments of the western Coastal Plain. Subaerial erosion along such near-surface fractures could have led to the development of the angular stream bends along the inner Coastal Plain. Many similar stream bends exist across the Cape Fear arch to the south, such as the conspicuous barbed bend in Livingston Creek along the Livingston Creek lineament (LCL) (Marple and Hurd 2021, fig. 11). The LCL and other nearby lineaments are located just northwest of the low-level seismicity near Wilmington (**Figure 1**). Studies of seismically induced paleoliquefaction deposits in the outer Coastal Plain of the Carolinas suggest that there could have been at least one prehistoric earthquake near the border between North and South Carolina (Weems and Obermeier 1990; Talwani and Schaeffer 2001). Thus, the LCL or other nearby lineament could be the surface expression of a buried active fault, displacement along which could have produced a large prehistoric earthquake. We, therefore, hypothesize that the angular stream bends along the inner Coastal Plain of northeastern North Carolina (**Figure 10**) formed by subaerial erosion along a broad zone of fractures associated with the RRFZ in the near-surface sediments.

The proposed RRFZ appears to have formed during the Cenozoic era since it crosscuts the Cretaceous and younger sedimentary formations beneath the Coastal Plain. The cumulative displacement along such a young fault zone in the eastern U.S. would be relatively small because of the low Cenozoic fault-slip rates in the eastern U.S. (0.3-1.5 m/my, Prowell 1988). Such a low-displacement strike-slip fault beneath the Coastal Plain would be difficult to detect using seismic-reflection, drill-hole, and potential field data. Furthermore, the only two closely spaced drill-holes near the RRL, WV-2-02 and WV-3-02 in **Figure 2a**, penetrated different sediments and therefore cannot be correlated across the RRL. Lastly, the alignment of the tilted part of the Roanoke River valley downstream from the RRL and the two topographic scarps bounding both sides of terrace A with the area of right-angle stream bends to the west (**Figures 4b** and **10**) suggests that the interpreted RRFZ is the principal displacement zone within a broad, at least 15-km-wide zone of faulting.

The alignment of the RRL with the Albemarle Sound to the east (**Figure 4**) suggests that the proposed RRFZ could continue ~80 km farther to the east. Subaerial erosion along the RRFZ in the outer Coastal Plain during the Pleistocene, when sea level was lower, could have formed the ancient Roanoke River valley beneath the sound.

Relative up-to-the-north displacement along the proposed RRFZ in the outer Coastal Plain is supported by the asymmetric drainage north of the Albermarle Sound where numerous tributaries drain this area (**Figure 4a**). Alternatively, this asymmetric drainage could be from Quaternary uplift to the north along other faults associated with the eastern Norfolk arch in northeastern North Carolina.

7.2 Origin of the circular topographic depressions, sand mounds, and circular patches of sand possibly associated with the RRL

7.2.1 Origin of the circular topographic depressions near the RRL

Various observations suggest that the small circular topographic depressions near the RRL (**Figures 5** and **13**) could be surface expressions of Holocene, seismically induced sandblows generated by earthquakes along the proposed RRFZ or other faults in the region. First, the circular depressions are similar in size and appearance to sandblows that formed during the 1886 Charleston, South Carolina, earthquake and the 1811-1812 New Madrid earthquakes in the northern Mississippi embayment of the central USA (e.g., Dutton 1889, plates XX and XXI; Fuller 1912, plate IXA). For example, LiDAR images of the Charleston, South Carolina, region show numerous similar depressions (Marple and Hurd 2020, figs. 4a, 7a, and 13a), which Marple and Hurd (2020) hypothesized could be surface expressions of sandblows that formed during large Holocene earthquakes in the Charleston region. Second, these depressions are concentrated in a belt located mostly north of the RRL (**Figure 5**). Third, the circular depressions do not appear to be Carolina bays because they are circular and lack sand rims (**Figure 13**). Nor do they appear to be gilgai (small shallow depressions associated with expanding and contracting clay soils; McManus 1999; Ahmed 2018) because they lack the necessary clay content for gilgai formation.

The small circular topographic depressions in the Roanoke River's floodplain south of the RRL (e.g., **Figure 12d**) may have formed differently from the other depressions north of the RRL. They could be from differential compaction of fine sediments dredged from the river by the USACE in the 1800s and 1900s. The finer sediments dredged from the channel would have flowed over the surrounding terrain. Differential compaction of these finer sediments could have then formed numerous shallow topographic depressions surrounding some of the sand mounds. Alternatively, some of the small depressions in the floodplain could represent holes dug along the edges of flat tar kilns for the tar-collecting barrels. Although tar kilns are commonly associated with soil mounds, one flat tar kiln was observed in the outer Coastal Plain northeast of Washington where the depression for the tar-collecting barrel (**Figure 6e**) is the only geomorphic evidence of the original tar kiln.

7.2.2 Origin of the patches of sand south of the lower Roanoke River valley

The light-colored patches of sand south of the lower Roanoke River valley (**Figure 14**) could represent the surface expressions of Holocene sandblows that have been leveled by farming practices in the region. Similar patches of sand are common throughout the New Madrid region of the central USA where large Holocene earthquakes have formed numerous sandblows and sand dikes, which have been leveled by modern farming practices in the northern Mississippi embayment (Tuttle *et al.* 2019).

7.2.3 Origin of the sand mounds along the Roanoke River's natural levees

The sand mounds along the Roanoke River's natural levees (**Figures 11** and **12**) are most likely sediments dredged from the channel by the USACE during the 1800s and 1900s for the following reasons. First, the USACE was commissioned to dredge the channel between Weldon and the Albemarle Sound (**Figure 1**) during the 19th and 20th centuries to make the river more navigable (Connolly 2023 written communication). Some of the dredging was carried out by pipeline dredging in which a perforated pipe was dragged across the landscape where the dredged sediments were deposited. Pipeline dredging could, therefore, explain the elongate shape and perpendicular orientation of most mounds relative to the riverbanks (**Figure 12a**). Second, the mounds are confined to the natural levees of the Roanoke River (**Figures 8 and 11**) rather than being randomly distributed across a much larger area, as would be expected of seismically induced liquefaction deposits (Tuttle *et al.* 2019). Third, the depressions along the mound axes are best explained by subsidence from dewatering of the dredged sediments or by the impact of the effluent exiting through holes in the pipeline during dredging operations. Four, the alternating pattern of mounds on opposite sides of the river (e.g., **Figure 11b**) is consistent with the deposition pattern expected from dredging. Five, the large volume of sand in each mound and the distribution of the mounds along the river's natural levees are inconsistent with seismically induced liquefaction (Tuttle *et al*. 2017). The removal of such large quantities of sand from the subsurface would have caused significant ground subsidence, which is not observed near the mounds. Lastly, the Roanoke River mounds closely resemble those along the natural levees of the Apalachicola River in Florida of the southeastern USA, which the USACE dredged from this river between 1957 and 2002 (Mossa *et al*. 2017). In both cases, the mounds exhibit elongate shapes and are restricted to the natural levees and nearby floodplains of both rivers, characteristics that are consistent with pipeline dredging.

7.3 Geological significance of the sand mounds along the Roanoke River

Although the USACE was commissioned to dredge the Roanoke River between Weldon and Albemarle Sound in the 1800s and 1900s, the sand mounds only occur south of the RRL. Here, most of the mounds are concentrated along the river's northeastern banks, opposite its southwestern valley wall where the channel is currently eroding sediments of the Yorktown Formation (**Figures 2a** and **11**). These observations suggest that the mound sediments originated primarily from channel deposits that the river eroded from its southwestern valley wall downstream from the RRL during Holocene time.

7.4 Re-evaluation of river anomalies along the ECFS-N in northeastern North Carolina

Several geomorphic observations support late Quaternary deformation along the interpreted ECFS-N in northeastern North Carolina. First, the prominent right-angle bend in Marsh Swamp and the abrupt transition from narrow, V-shaped valleys along Fishing Creek and the Tar River west of the ECFS-N to broad floodplains downstream (**Figure 2a**) are best explained by up-to-the-west, late Quaternary transpressional uplift and subaerial erosion along fractures in the near-surface sediments along the interpreted ECFS-N. Second, the localized incision along Fishing Creek and the Tar River where they cross the ECFS-N (Marple and Talwani 2000) supports gentle Holocene transpressional uplift along this trend. Third, the greater drainage density and dry, elevated nature of Burnt Coat Swamp northwest of Marsh Swamp (**Figures 2a** and **15**) indicate that the northwestern side of Marsh Swamp has been gently uplifted at least 1-2 m relative to the southeastern side of the swamp during the Holocene. The local narrowing of the Beaverdam and Burnt Coat swamps and the Fishing Creek valley ("pinched" valleys) on the western (upstream) side of the ECFS-N (**Figure 2a**) further support transpressional uplift along the ECFS-N (Howard 1967). Thus, the right-angle bend along Marsh Swamp and the abrupt widening of the Tar River and Fishing Creek valleys downstream from this trend of geomorphic anomalies likely formed by subaerial erosion and up-to-the-west, late Quaternary transpressional uplift along the interpreted ECFS-N.

In contrast to our hypothesis, Weems *et al.* (2009) postulated that the right-angle bend along Marsh Swamp and the abrupt widening of the Fishing Creek valley floor to the southwest (**Figure 2a**) developed by subaerial erosion along joints in the near-surface sediments of the Yorktown Formation. They attributed the formation of these joints to Neogene reactivation of the Whitakers and Palmyra faults (**Figure 2a**). Joints, however, are non-displacement fractures and therefore cannot explain the evidence for local uplift along this trend of geomorphic anomalies.

7.5 Evidence for the Tar River right-step releasing offset (TRO) and its possible association with the RRL

The gentle bend in the RRL near Palmyra toward the TRO (**Figure 1**) suggests that the interpreted RRFZ may have formed to accommodate the dilatational change in volume caused by extension at the TRO (**Figure 16**). However, unlike releasing steps along plate boundary strike-slip faults (Cunningham and Mann 2007), the TRO lacks an extensional basin. The absence of such a basin likely results from the low fault slip rates in the eastern U.S. (0.3-1.5 m/my, Prowell 1988) and the interpreted Quaternary age of the ECFS. If true, the total dextral strike-slip displacement along the ECFS during the Cenozoic would have been only a few tens of meters, which is too small to have formed a deep extensional basin at the TRO. Despite the lack of a basin at the TRO, the southward-convex curve in the Tar River north of the TRO (**Figure 16**) suggests that gentle subsidence at the TRO could have caused the Tar River to locally migrate southward toward the TRO. Further studies are needed though to confirm this hypothesis.

7.6 Origin of the Tar River's WSW migration southeast of Tarboro

We hypothesize that the Tar River's WSW migration southeast of Tarboro (**Figure 1**) was produced by a down-to-the-WSW cross-valley tilt associated with transtension along the south side of a curve in a sinistral strike-slip fault, herein named the Tarboro fault. We interpret the Tarboro fault based on the alignment of the bend in the Tar River southeast of Tarboro with the scarp along the southern edge of terrace A (**Figure 4b**). The small historical earthquake northeast of the river bend (**Figure 10**) supports continued deformation along this proposed fault. Sinistral displacement along this interpreted fault is favored by its oblique orientation relative to S_{Hmax} (**Figure 16**). We propose that late Quaternary sinistral displacements along the curved portion of the interpreted Tarboro fault caused transtension south of this fault curve (**Figure 16**). Such down-to-the-WSW tilting of the terrain south of this fault curve could have caused the Tar River southeast of Tarboro to migrate to the west-southwest during late Pleistocene-Holocene time. This mechanism of cross-valley tilting is like that proposed herein south of the bend in the interpreted western RRFZ near Palmyra (**Figure 16**). Further studies are needed though to confirm this hypothesis.

7.7 Origin of the Corduroy Swamp lineament (CSL)

The Corduroy Swamp lineament (CSL) appears to be associated with a buried sinistral strike-slip fault, herein named the Corduroy Swamp fault (CSF), based on the following observations. First, the linear nature of the Corduroy Swamp along the CSL differs from the dominant dendritic stream pattern in the Coastal Plain (**Figure 4a**). Second, the southwest migration of the ancestral Roanoke River away from this area since the early Pleistocene (Weems *et al.* 2009) suggests that early Pleistocene transpressional uplift along the proposed CSF caused the ancestral Roanoke River to migrate southwestward away from the CSF. The large eastward projection of the late Pliocene Varina Grove unit (Tbv) along the CSL (**Figure 2a**) suggests that the uplift along the proposed CSF may have begun earlier during late Pliocene time. If true, late Pliocene to Holocene transpressional uplift along the interpreted CSF could be responsible for Quaternary uplift along the western Norfolk arch. Similar geomorphic features occur along the NW-SE-oriented Faison and Jarmantown lineaments that cross the Cape Fear arch to the south (**Figure 1**). Marple and Hurd (2021) hypothesized that

these two lineaments originated from late Quaternary deformation along the interpreted Faison and Neuse faults beneath the Coastal Plain of southeastern North Carolina.

7.8 Low-level seismicity along the interpreted faults beneath the Coastal Plain of northeastern North Carolina

Although the ENE-WSW orientation of S_{Hmax} favors displacements along the various faults interpreted herein, little or no historical seismicity has occurred along any of them (**Figure 1**). This lack of seismicity is likely due to the low strain rate along the Atlantic margin (10^{-9} to 10^{-10} $^{yr-1}$, Johnston 1989), which favors long recurrence intervals between large earthquakes along active faults beneath the U.S. Atlantic Coastal Plain. Numerous studies of intraplate faults in the central and eastern USA have documented evidence for late Quaternary deformation along these faults where little modern seismicity has been recorded. Examples of such faults include the Meers fault in southwestern Oklahoma (Crone and Luza 1990), the Bootheel fault in southeastern Missouri (Marple and Schweig 1992; Guccione *et al*. 2005), the Graingers fault zone summarized herein (**Figure 1**), the Saline River fault zone in southeastern Arkansas (Cox *et al*. 2012), the interpreted Livingston Creek, Faison, and Neuse faults that cross the Cape Fear arch in southeastern North Carolina (Marple and Hurd 2021), and the interpreted southwest continuation of the Norumbega fault system in southern New England (Marple and Hurd 2019). Furthermore, studies of seismically induced liquefaction deposits in southeastern North Carolina and northeastern South Carolina (Weems and Obermeier 1990; Talwani and Schaeffer 2001) show evidence for at least one large prehistoric earthquake that could have occurred along a fault near the border between North and South Carolina where little modern seismicity has been recorded (**Figure 1**), like that in the Iranian Coastal Makran (Kaveh-Firouz *et al.* 2023a). Studies of intraplate faults elsewhere in the world, such as those in the Central Iranian Plateau (Kaveh-Firouz *et al.* 2023b) and those associated with the Marryat and Tennant Creek earthquakes in Australia (Crone *et al*. 1997), have also shown that intraplate faults can be aseismic for long periods of time between large earthquakes. If true, the low-level seismicity along the interpreted faults beneath the North Carolina Coastal Plain could be a poor indicator of their seismogenic potential.

8. Summary and conclusions

The geomorphic anomalies that define the Roanoke River lineament (RRL), combined with its oblique, E-W orientation relative to the ENE-WSW-oriented S_{Hmax} (**Figure 16**), suggest that it is associated with a buried, potentially active sinistral strike-slip fault zone, herein named the Roanoke River fault zone (RRFZ), beneath the Coastal Plain of northeastern North Carolina. The broad zone of angular stream bends and rectilinear topographic depressions along the inner Coastal Plain to the west (**Figures 7** and **10**) suggests that the proposed RRFZ could be associated with a broad zone of faulting at least 15 km wide. Increased incision along the Roanoke River upstream from the RRL (**Figure 8a**, profiles 1-5), the monoclinal scarp along the eastern RRL (**Figure 5**), and the absence of surficial unit Qalb in the Roanoke River valley south of the RRL (**Figure 2a**) suggest that the interpreted RRFZ has undergone Holocene, up-to-the-north displacements beneath the Coastal Plain. The bend in the interpreted RRFZ toward the Tar River right-step releasing offset (TRO) along the ECFS suggests that the RRFZ could have formed to accommodate the dilatational change in volume associated with Quaternary extension at the TRO to the southwest (**Figure 16**).

Unlike releasing steps along plate boundary strike-slip faults (Cunningham and Mann 2007), the TRO lacks an extensional basin. The absence of a deep basin at the TRO likely results from the low cumulative slip along the ECFS, which is inferred from the low fault slip rates in the eastern U.S. (0.3-1.5 m/my, Prowell 1988) and the interpreted Quaternary age of the ECFS. Despite the lack of an extensional basin at the TRO, the southward-convex curve in the Tar River toward the TRO (**Figure 16**) supports Quaternary subsidence at the

TRO, which could have caused this river to locally migrate southward toward the TRO. Detailed studies of the TRO and ECFS using LiDAR and subsurface data are needed though to confirm this hypothesis.

Sinistral strike-slip motion along the bend in the RRFZ near Palmyra during Holocene time favored transtension along this fault bend (**Figure 16**). We suggest that this transtension caused the terrain south of the fault bend to tilt down-to-the-SW, thereby causing this part of the Roanoke River to migrate southwestward during Holocene time. We postulate that the Tar River's WSW migration southeast of Tarboro (**Figure 1**) was also produced by transtension south of the curve in the interpreted Tarboro strike-slip fault (**Figure 16**). Sinistral displacement along this fault bend, like that along the interpreted bend in the RRFZ, during late Pleistocene-Holocene time could have caused the Tar River south of the Tarboro fault bend to migrate to the west-southwest. Further studies are needed though to confirm these hypotheses.

The geomorphic anomalies that define the Corduroy Swamp lineament (CSL), combined with its oblique, E-W orientation relative to the ENE-WSW-oriented S_{Hmax} (**Figure 16**), suggest that it is associated with a buried, potentially active, transpressional sinistral strike-slip fault, herein named the Corduroy Swamp fault (CSF), beneath the Coastal Plain of northeastern North Carolina. The southwestward migration of the early Pleistocene Roanoke River away from the interpreted CSF and the eastward projection of late Pliocene-Pleistocene surficial geologic units along the CSL (**Figure 2a**) suggest that late Pliocene-Pleistocene uplift along the proposed CSF could be responsible for late Quaternary uplift along the western Norfolk arch.

Despite the evidence for late Quaternary deformation along the proposed RRFZ, ECFS, CSF, and GFZ, little or no seismicity has occurred along these interpreted faults (**Figure 1**). However, studies of intraplate faults elsewhere have shown that intraplate faults can be aseismic for long periods of time between large earthquakes (e.g., Crone *et al*. 1997). If true, the low-level seismicity along these interpreted faults could be a poor indicator of their seismogenic potential.

Further geological and geophysical studies, including seismic-reflection profiling, ground penetrating radar (GPR), and drill-hole data, are needed to determine if large damaging earthquakes could someday occur along the interpreted faults beneath the North Carolina Coastal Plain. Further studies are also needed to determine if the small circular topographic depressions near the RRL (**Figures 5** and **13**) and the patches of sand south of the lower Roanoke River valley (**Figure 14**) are surface expressions of seismically induced paleoliquefaction, including GPR, trenching, drill-hole data, and shallow electrical resistivity surveys. A large earthquake today in eastern North Carolina could cause tremendous damage and loss of life. Fayetteville, Smithfield, Rocky Mount, and Roanoke Rapids, for example, lie along the ECFS while Kinston and Greenville are located near the GFZ. Further studies of the faults proposed herein could also help to better understand the tectonic development of the Albemarle embayment and Norfolk arch along the U.S. Atlantic continental margin.

Acknowledgements

The authors wish to thank the anonymous reviewers for their thoughtful and constructive comments that helped to improve this paper.

Conflict of interest

The authors declare no conflict of interest.

References

1. Ahmed, M.Y. 2018. The influence of roadside vegetation on pavement roughness affected by alluvial expansive soil deposits in Victoria, Australia. Swinburne University of Technology, Melbourne, Australia, 131 p.

2. Ator, S.W., Denver, J.M., Krantz, D.E., Newell, W.L., and Martucci, S.K. 2005. A surficial hydrogeologic framework for the mid-Atlantic Coastal Plain. U.S. Geological Survey, Professional Paper 1680, 44 p., 4 sheets, scale 1:100 000.
3. Brown, P.M., Brown, D.L., Shufflebarger, T.E., Jr., and Sampair, J.L. 1977. Wrench-style deformation in rocks of Cretaceous and Paleocene age, North Carolina Coastal Plain. North Carolina Department of Natural and Economic Resources, Division of Earth Resources, Special Publication 5, Raleigh, North Carolina, 47 p.
4. Brown, P.M., Shufflebarger, T.W., Jr., and Smith, S.R. 1982. Structural-stratigraphic framework and geomorphic signature of the Graingers wrench zone, North Carolina Coastal Plain. Atlantic Coastal Plain Geological Association, 1982 Field Trip Guidebook, 34 p.
5. Brown, P.M., Burt, E.R., III, Carpenter, P.A., III, Enos, R.M., Flynt, B.J., Jr., Gallagher, P.E., Hoffman, C.W., Merschatt, C.E., Wilson, W.F., and Parker, J.M., III. 1985. Geologic map of North Carolina. North Carolina Department of Natural Resources and Community Development, Raleigh, North Carolina, 1 sheet, scale 1:500 000.
6. Carter, M.W. and McLaurin, B.T. 2019. Paleoliquefaction field reconnaissance in eastern North Carolina−Is there evidence for large magnitude earthquakes between the Central Virginia seismic zone and Charleston seismic zone? U.S. Geological Survey, Scientific Investigations Report 2019-5057, 54 p. https://doi.org/10.3133/sir20195057
7. Colquhoun, D.J., Johnson, G.G., Peebles, P.C., Huddlestun, P.F., and Scott, T. 1991. Quaternary geology of the Atlantic Coastal Plain. *In* Quaternary nonglacial geology: Conterminous U.S.: Geology of North America. *Edited by* R.B. Morrison. Geological Society of America, Boulder, Colorado, K-2, pp. 629-650. https://doi.org/10.1130/DNAG-GNA-K2.629
8. Cox, R.T., Harris, J., Forman, S., Brezina, T., Gordon, J., Gardner, C., and Machin, S. 2012. Holocene faulting on the Saline River fault zone, Arkansas, along the Alabama-Oklahoma transform. *In* Recent advances in North American paleoseismology and neotectonics east of the Rockies. *Edited by* R.T. Cox, M.P. Tuttle, O.S. Boyd, and J. Locat. Geological Society of America, Special Paper 493, pp. 17-36. doi:10.1130/2012.2493(07)
9. Crone, A.J. and Luza, K.V. 1990. Style and timing of Holocene surface faulting on the Meers fault, southwestern Oklahoma. Geological Society of America Bulletin, 102, pp. 1-17.
10. Crone, A.J., Machette, M.N., and Bowman, J.R. 1997. Episodic nature of earthquake activity in stable continental regions revealed by paleoseismicity studies of Australian and North American Quaternary faults. Australian Journal of Earth Science, 44, no. 2, pp. 203-214. https://doi.org/10.1080/08120099708728304
11. Cronin, T.M. 1981. Rates and possible causes of neotectonic vertical crustal movements of the emerged southeastern United States Atlantic Coastal Plain. Geological Society of America Bulletin, part 1, 92, pp. 812-833.
12. Cronin, T.M., Bybell, L.M., Poore, R.Z., Blackwelder, B.W., Liddicoat, J.C., and Hazel, J.E. 1984. Age and correlation of emerged Pliocene and Pleistocene deposits, U.S. Atlantic Coastal Plain. Palaeogeography, Palaeoclimatology, Palaeoecology, 47, pp. 21-51.
13. Cunningham, W.D. and Mann, P. (*Editors*). 2007. Tectonics of strike-slip restraining and releasing bends. Geological Society of London, Special Publications Number 290, 482 p. https://doi.org/10.1144/SP290.0
14. Daniels, D.L. and Zietz, I. 1978. Geologic interpretation of aeromagnetic maps of the Coastal Plain region of South Carolina and parts of North Carolina and Georgia. U.S. Geological Survey, Open-File Report 78-261, 47 p. plus appendix.
15. Dutton, C.E. 1890. The Charleston earthquake of August 31, 1886. U.S. Geological Survey, Extract from the Ninth Annual Report of the Director, 1887-‘88, Reprinted 1979, Government Printing Office, Washington, D.C., pp. 203-528
16. Fuller, M.L. 1912. The New Madrid earthquake. U.S. Geological Survey, Bulletin 494, 120 p.
17. Gay, N.M. 2004. The bedrock geology of the western portion of the Rocky Mount 100K quadrangle, Nash, Wilson, and Edgecombe counties, North Carolina. North Carolina Geological Survey, Open File Report 2004-05, scale 1:50 000.
18. Gayes, P.T., Nelson, D.D., and Ward, T. 1992. Ancestral channels of the ancient Pee Dee River on the inner continental shelf off Murrels Inlet. South Carolina Geology, 34, nos. 1 and 2, pp. 53-56.
19. Glass, C.E. and Slemmons, D.B. 1978. State of the art for assessing earthquake hazards in the United States. Report 11, Imagery in earthquake analysis: Vicksburg, Mississippi, U.S. Army Corps of Engineers Waterways Experiment Station, Miscellaneous Paper S-73-1, 221 p.
20. Gohn, G.S. 1988. Late Mesozoic and early Cenozoic geology of the Atlantic Coastal Plain: North Carolina to Florida. *In* The Atlantic continental margin U.S.: Geology of North America. *Edited by* R.E. Sheridan and J.A. Grow. Geological Society of America, Boulder, Colorado, pp. 107-130.
21. Guccione, M., Marple, R., and Autin, W. 2005. Evidence for Holocene displacements along the Bootheel fault (lineament) in southeastern Missouri: Seismotectonic implications for the New Madrid region. Geological Society of America Bulletin, 117, no. 3/4, pp. 319-333.
22. Harris, W.B., Zullo, V.A., and Baum, G.R. 1979. Tectonic effects on Cretaceous, Paleogene, and early Neogene sedimentation, North Carolina. *In* Structural and stratigraphic framework for the Coastal Plain of North Carolina.

Edited by G.R. Baum, W.B. Harris, and V.A. Zullo. Carolina Geological Society and Atlantic Coastal Plain Geological Association Field Trip Guidebook, October, 1979, Wrightsville Beach, North Carolina, pp. 19-29.
23. Harrup, M. 2013. [unpublished Masters thesis] Tar kilns of Goose Creek State Park: History and preservation. East Carolina University, Greenville, North Carolina, 106 p. https://www.thescholarship.ecu.edu/bitstream/handle/10342/1816/Harrup_ecu_0600M_10943.pdf?sequence=1&isAllowed=y
24. Horton, J.W., Jr., Drake, A.A., Jr., and Rankin, D.W. 1989. Tectonostratigraphic terranes and their Paleozoic boundaries in the central and southern Appalachians. *In* Terranes in the circum-Atlantic Paleozoic orogens. *Edited by* R.D. Dallmeyer. Geological Society of America, Special Paper 230, pp. 213-245.
25. Howard, A.D. 1967. Drainage analysis in geologic interpretation: A summation. The American Association of Petroleum Geologists Bulletin, 51, no. 11, pp. 2246-2259.
26. Johnston, A.C. 1989. The seismicity of "stable continental interiors." *In* Earthquakes at North Atlantic passive margins: Neotectonics and postglacial rebound. *Edited by* S. Gregersen and P.W. Basham. Kluwer Academic Publishers, Dordrecht, Netherlands. NATO ASI Series C: Mathematical and Physical Sciences, 266, pp. 299-327.
27. Kaveh-Firouz, A., Burg, J.P., and Giachetta, E. 2024. Landscape evolution in orogenic plateaus: Insights from quantitative morphotectonic analysis of the Turkish–Iranian Plateau and Caucasus regions. Earth Surface Processes and Landforms, 49, no. 3, pp. 1214-1238. https://doi.org/10.1002/esp.5756
28. Kaveh-Firouz, A., Burg, J.P., Haghipour, N., Mandal, S.K., Christl, M., and Mohammadi, A. 2023a. Tectonics, base-level fluctuations, and climate impact on the Eocene to present-day erosional pattern of the Arabia-Eurasia collision zone (NNW Iranian Plateau and west Alborz Mountains). Tectonics, 42, no. 8, Article ID. e2022TC007684, 29 p. https://doi.org/10.1029/2022TC007684
29. Kaveh-Firouz, A., Mohammadi, A., Görüm, T., Sarıkaya, M.A., Alizadeh, H., Akbaş, A., and Mirarabi, A. 2023b. Main drivers of drainage pattern development in onshore Makran Accretionary Wedge, SE Iran. International Journal of Earth Sciences, 112, no. 2, pp. 539-559. https://doi.org/10.1007/s00531-022-02270-6
30. Kohler, M. 1976. Lenoir County: 200 years of progress: A report of history and achievements of Lenoir County: Kinston, North Carolina Bicentennial Commission and Lenoir County Board of Commissioners, 160 p.
31. Lawrence, D.P. and Hoffman, C.W. 1993. Geology of basement rocks beneath the North Carolina Coastal Plain. North Carolina Geological Survey, Bulletin 95, 60 p.
32. Lundstern, J. and Zoback, M.D. 2020. Multiscale variations of the crustal stress field throughout North America. Nature Communications, 11, no. 1951. https://doi.org/10.1038/s41467-020-15841-5
33. Markewich, H.W. 1985. Geomorphic evidence for Pliocene-Pleistocene uplift in the area of the Cape Fear arch, North Carolina. *In* Tectonic geomorphology. *Edited by* M. Morisawa and J.T. Hack. Proceedings, 15th Annual Binghamton Geomorphology Symposium. Allen and Unwin, Boston, Massachusetts, pp. 279–297.
34. Marple, R.T. 1994. [unpublished Ph.D. dissertation] Discovery of a possible seismogenic fault system beneath the Coastal Plain of South and North Carolina from an integration of river morphology and geological and geophysical data. University of South Carolina, Columbia, 354 p.
35. Marple, R.T. and Hurd, J.D., Jr. 2019. LiDAR and other evidence for the southwest continuation and late Quaternary reactivation of the Norumbega Fault System and a cross-cutting structure near Biddeford, Maine, USA. Atlantic Geology, 55, pp. 323-359.
36. Marple, R.T. and Hurd, J.D., Jr. 2020. Interpretation of lineaments and faults near Summerville, South Carolina, USA, using LiDAR data: Implications for the cause of the 1886 Charleston, South Carolina, earthquake. Atlantic Geology, 56, pp. 73-95.
37. Marple, R.T. and Hurd, J.D., Jr. 2021. Investigation of the Cape Fear arch and East Coast fault system (ECFS) in the Coastal Plain of North Carolina and northeastern South Carolina, USA, using LiDAR data. Atlantic Geology, 57, pp. 311-341.
38. Marple, R.T. and Hurd, J.D., Jr. 2022. Further evidence for the East Coast fault system and faults associated with the Summerville restraining bend and their possible relationship to the 1886 Charleston earthquake, South Carolina, USA. Atlantic Geoscience, 58, pp. 99-129. doi:10.4138/atlgeo.2022.004
39. Marple, R.T. and Schweig, E.S., III. 1992. Remote sensing of alluvial terrain in a humid, tectonically active setting: "The New Marid Seismic Zone". Photogrammetric Engineering and Remote Sensing, 58, no. 2, pp. 209-219.
40. Marple, R.T. and Talwani, P. 2000. Evidence for a buried fault system in the Coastal Plain of the Carolinas and Virginia−Implications for neotectonics in the southeastern United States. Geological Society of America Bulletin, 112, no. 2, pp. 200-220.
41. McLaurin, B.T. and Harris, W.B. 2001. Paleocene faulting within the Beaufort Group, Atlantic Coastal Plain, North Carolina. Geological Society of America Bulletin, 113, no. 5, pp. 591-603. doi.org/10.1130/0016-7606(2001)113<0591:PFWTBG>2.0.CO;2

42. McManus, K. 1999. Mound theory, gilgai and PSD analysis. *In* Proceedings, 8th Australia New Zealand Conference on Geomechanics: Consolidating Knowledge. *Edited by* N.D. Vitharana and R. Colman. Australian Geomechanics Society. Hobart, Australian Capital Territory, pp. 195-199.
43. Moore, C.R. and Daniel, I.R., Jr. 2011. Geoarchaeological investigations of stratified sand ridges along the Tar River, North Carolina. *In* The Archaeology of North Carolina: Three Archaeological Symposia. North Carolina Archaeological Council, Publication Number 30. *Edited by* C.R. Ewen, T.W. Whyte, and R.P.S. Davis, Jr., 44 p.
44. Moore, C.M., Brooks, M.J., Mallinson, D.J., Parham, P.R., Ivester, A.H., and Feathers, J.K. 2016. The Quaternary evolution of Herndon Bay, a Carolina bay on the Coastal Plain of North Carolina (USA): Implications for paleoclimate and oriented lake genesis. Southeastern Geology, 51, no. 4, pp. 145-171.
45. Mossa, J., Chen, Y., Walls, S., Kondolf, G., and Wu, C. 2017. Anthropogenic landforms and sediments from dredging and disposing sand along the Apalachicola River and its floodplain. Geomorphology, pp. 119-134. https://doi.org/10.1016/j.geomorph.2017.03.010
46. Nazari, H., Ritz, J.F., Walker, R.T., Salamati, R., Rizza, M., Patnaik, R., Hollingsworth, J., Alimohammadian, H., Jalali, A., Firouz, A.K., and Shahidi, A. 2014. Palaeoseismic evidence for a medieval earthquake, and preliminary estimate of late Pleistocene slip-rate, on the Firouzkuh strike-slip fault in the Central Alborz region of Iran. Journal of Asian Earth Sciences, 82, pp. 124-135. https://doi.org/10.1016/j.jseaes.2013.12.018
47. NOAA Office for Coastal Management. 2015. North Carolina Floodplain Mapping Program (NCFMP) Lidar: Statewide North Carolina (Phases 1 and 2), Charleston, South Carolina. https://www.coast.noaa.gov/digitalcoast//contributing-partners/ncfmp.html
48. O'Driscoll, M., Johnson, P., and Mallinson, D. 2010. Geological controls and effects of floodplain asymmetry on river-groundwater interactions in the southeastern Coastal Plain, USA. Hydrogeology Journal, 18, pp. 1265-1279.
49. Oliva, M., Palacios, D., Sancho, L.G., Fernández-Fernández, J.M., Çiner, A., Fernandes, M., García-Oteyza, J., Sarıkaya, M.A., Serrano, E., Kaveh-Firouz, A., and Pérez-Alberti, A. 2024. The origin of the ice-free areas of the Hurd Peninsula (Livingston Island, Antarctica). Quaternary Science Reviews, 344, Article ID 108991, 28 p. https://doi.org/10.1016/j.quascirev.2024.108991
50. Ouchi, S. 1985. Response of alluvial rivers to slow active tectonic movement. Geological Society of America Bulletin, 96, no. 4, pp. 504-515. https://doi.org//10.1130/0016-7606(1985)96<504:ROARTS>2.0.CO;2
51. Peri, V.G., Haghipour, N., Christl, M., Terrizzano, C., Kaveh-Firouz, A., Leiva, M.F., Pérez, P., Yamin, M., Barcelona, H., and Burg, J.P. 2022. Quaternary landscape evolution in the Western Argentine Precordillera constrained by 10Be cosmogenic dating. Geomorphology, 396, Article ID 107984. https://doi.org/10.1016/j.geomorph.2021.107984
52. Prowell, D.C. 1983. Index of faults of Cretaceous and Cenozoic age in the eastern United States. U.S. Geological Survey, Miscellaneous Field Studies Map MF-1269, 1 sheet, scale 1:2 500 000.
53. Prowell, D.C. 1988. Cretaceous and Cenozoic tectonism on the Atlantic coastal margin. *In* The Atlantic continental margin U.S.: Geology of North America. *Edited by* R.E. Sheridan and J.A. Grow. Boulder, Colorado, I-2, pp. 557-564.
54. Reager, B.G., Stover, C.W., and Algermissen, S.T. 1987. Seismicity map of the state of North Carolina. U.S. Geological Survey, Miscellaneous Field Studies Map MF-1988, Revised edition of MF 1224, scale 1:1 000 000.
55. Richardson, C.J. (*Editor*). 1981. Pocosin wetlands. Hutchinson Ross Publishing Company, Stroudsburg, Pennsylvania, 364 p.
56. Sampair, J.L. 1979. Geological and geophysical evaluation of the Graingers basin for Triassic sediments. North Carolina Geological Survey, Open File Report 79-1, 37 p.
57. Schumm, S.A., Dupont, J.F., and Holbrook, J.M. 2000. Active tectonics and alluvial rivers. Cambridge University Press, Cambridge, UK, New York, NY, 276 p.
58. Schwartz, S.Y., Orange, D.L., and Anderson, R.S. 1990. Complex fault interactions in a restraining bend on the San Andreas fault, southern Santa Cruz Mountains, California. Geophysical Research Letters, 17, no. 8, pp. 1207-1210.
59. Snitker, G., Moser, J.D., Southerlin, B., and Stewart, C. 2022. Detecting historic tar kilns and tar production sites using high-resolution, aerial LiDAR-derived digital elevation models: Introducing the Tar Kiln Feature Detection workflow (TKFD) using open-access R and FIJI software. Journal of Archaeological Science, Reports, 41. https://doi.org/10.1016/j.jasrep.2022.103340
60. Soller, D.R. 1983. [unpublished Ph.D. dissertation] The Quaternary history and stratigraphy of the Cape Fear River valley. George Washington University, St. Louis, Missouri, 192 p.
61. Soller, D.R. 1988. Geology and tectonic history of the lower Cape Fear River valley, southeastern North Carolina. U.S. Geological Survey, Professional Paper 1466-A, 60 p.
62. Soller, D.R. and Mills, H.H. 1991. Surficial geology and geomorphology. *In* The geology of the Carolinas: 50th Anniversary Volume. *Edited by* J.W. Horton Jr. and V.A. Zullo. The University of Tennessee Press, Knoxville, Tennessee, pp. 290-308.
63. Stein, R.S. and Yeats, R.S. 1989. Hidden earthquakes. Scientific American, 260, no. 6, pp. 48-57.

64. Talwani, P. and Schaeffer, W.T. 2001. Recurrence rates of large earthquakes in the South Carolina Coastal Plain based on paleoliquefaction data. Journal of Geophysical Research, 106, pp. 6621-6642. https://doi.org/10.1029/2001JB900398
65. Tuttle, M.P., Villamor, P., Almond, P., Barrett n. Bastin, S., Bucci, M.G., Landridge, R., Clark, K., and Hardwick, C.M. 2017. Liquefaction induced during the 2010-2011 Canterbury, New Zealand, earthquake sequence and lessons learned for the study of paleoliquefaction features. Seismological Research Letters, 88, no. 5, pp. 1403-1414 plus electronic supplement. doi:10.1785/0220170073
66. Tuttle, M.P., Hartleb, R., Wolf, L., and Mayne, P.W. 2019. Paleoliquefaction studies and the evaluation of seismic hazard. Geosciences, 9, no. 7, 61 p. doi:10.3390/geosciences9070311
67. U.S. Geological Survey. 2022. Earthquake Hazards Program. M2.1 earthquake 24 June 2013 – 13 km SSW of Kinston, North Carolina. https://earthquake.usgs.gov/earthquakes/eventpage/se06243a/executive. Retrieved 1 October 2022.
68. U.S. Geological Survey. 2025. Earthquake Hazards Program. https://earthquake.usgs.gov/earthquakes/eventpage/se606232/map. Retrieved 27 January 2025.
69. Weems, R.E. and Lewis, W.C. 2007. Detailed sections from auger holes in the Roanoke Rapids 1:100 000 map sheet. U.S. Geological Survey, Open-File Report 2007-1092, 155 p.
70. Weems, R.E. and Obermeier, S.F. 1990. The 1886 Charleston earthquake: An overview of geological studies. *In* Proceedings of the 17th Water Reactor Safety Information Meeting: NUREG/CP-0105, 2, pp. 289-313, Nuclear Regulatory Commission, Washington, D.C.
71. Weems, R.E., Lewis, W.C., and Aléman-Gonzalez, W.B. 2009. Surficial geologic map of the Roanoke Rapids 30' x 60' quadrangle, North Carolina. U.S. Geological Survey, Open-File Report 2009-1149, 1 sheet, scale 1:100 000.
72. Weems, R.E., Self-Trail, J.M., and Edwards, L.E. 2019. Cross section of the North Carolina Coastal Plain from Enfield through Cape Hatteras. U.S. Geological Survey, Open-File Report 2019-1145, 2 sheets.
73. Withjack, M.O., Malinconico, M.L., and Durcanin, M. 2020. The "passive" margin of eastern North America: Rifting and the influence of prerift orogenic activity on postrift development. Lithosphere, 82, Article ID 8876280, 29 p. https://doi.org/10.2113/2020/8876280

Figure captions

Figure 1. Diagram showing the Roanoke River (RRL) and Corduroy Swamp (CSL) lineaments and the Tar River right-step releasing offset (TRO) along the ECFS. The gray pattern is the area of faults (black lines) crossing the Cape Fear arch interpreted by Marple and Hurd (2021). ABS is the Albemarle Sound. Red star labeled 1 shows the location of a M 2.1 earthquake near the Graingers fault zone (GFZ) in 2013 (U.S. Geological Survey 2022). Red dots in North Carolina are small (≥MMI III) historical earthquakes between 1735 and 1983 (Reager *et al*. 1987) while the red dots in South Carolina are small (M ≥ 3.0), instrumentally recorded earthquakes of the U.S. Geological Survey (2025). Black triangles are seismically induced paleoliquefaction sites of Talwani and Schaeffer (2001). WSW-pointing arrows along the lower Tar River valley show the area of the river's WSW migration during late Pleistocene-Holocene time. S_{Hmax} (opposing arrows) is the orientation of the regional maximum horizontal compressive stress field (Lundstern and Zoback 2020). Striped pattern labeled SFs at the northern end of the ECFS-S represents the area of surface faults summarized in Prowell (1983). CRB is the Cape Fear restraining bend along the ECFS-S (Marple and Hurd 2021). Short-dashed pattern is the buried Graingers basin (GB). The red dashed contour shows the locations of the Albemarle embayment (AE), Cape Fear arch (CFA), and Norfolk arch (NFA).

Figure 2. (a) Portion of the surficial geologic map of Weems *et al*. (2009) with the ECFS-N, RRL, and CSL (dashed lines) overlain. Faults are shown as short-dashed lines. Red contours are structure contours (100 ft interval) drawn on the base of the Coastal Plain sediments. BCS and BVS are the Burnt Coat and Beaverdam swamps, respectively. PV shows the locations of narrowed (pinched) valleys along the Burnt Coat and Beaverdam swamps and the Tar River valley. Qal2 is a low terrace that represents older Holocene valley sediments in which the modern floodplain (unit Qal) has become entrenched (Figure 8, profile 5). **(b)** Conceptual geological cross-section (not to scale) showing how the interpreted Roanoke River and Tarboro faults cut through the pre-Cretaceous crystalline basement and deeper Coastal Plain sediments in the eastern part of the study area. Folding of the shallower sediments occurs above the fault tip in the deeper Coastal Plain to the east. In this conceptual model the Roanoke River fault zone is the principal displacement zone within a broader zone of secondary faults shown by vertical dashed lines. The dip direction of all interpreted faults is unknown.

Figure 3. (a) Photograph of deep incision along the Cape Fear River near Erwin, North Carolina, caused by Late Pleistocene-Holocene uplift along the ECFS-S just to the southeast. Notice the two-story house behind several trees on the ~40-ft-high bluff overlooking the river. **(b)** The Cape Fear River near Lillington, ~15 km upstream from photo (a) where the river is only 5-10 feet (2-3 m) below its banks. This observation is opposite that expected for Coastal Plain rivers. Without local uplift along the ECFS-S, the Cape Fear River would be expected to be less incised here than upstream near Lillington to the northwest. Also note the rapids (Smiley's Falls) in photo (a) formed by an erosionally resistant metavolcanic epi-clastic rock (unit CZve) of the Eastern Slate Belt (Brown *et al*. 1985), suggesting that uplift along the ECFS-S has uplifted and exposed this metamorphic rock along the Cape Fear River. Photos taken 1 March 2024.

Figure 4. (a) Color LiDAR image across the Albemarle embayment of northeastern North Carolina. Illumination azimuth is 140º. RRL is the Roanoke River lineament. The Roanoke River is highlighted in black. Arrows point toward angular stream bends. CS, MR, MS,

PC, and WR are Corduroy Swamp, Meherrin River, Marsh Swamp, Potecasi Creek, and Wiccacon River. Opposing arrows labeled TH show the topographically high area that partly defines the CSL. H, J, P, T, and W are the towns Hamilton, Jamesville, Palmyra, Tarboro, and Weldon. Lines labeled 1-9 are elevation profile locations shown in Figures 8a and 8b. **(b)** IHS-enhanced version of image (a). The E-W-oriented, 8- to 10-km-wide green pattern labeled A is terrace A described in the text. The Roanoke River is highlighted in white. WSW-pointing arrows labeled SW along the lower Tar River valley show the river's area of WSW migration during late Pleistocene-Holocene time. Image locations are shown in Figure 1.

Figure 5. Enlarged color LiDAR image showing the E-W-oriented monoclinal-like scarp, southwest deflection of the Roanoke River, and angular stream bends (arrows) to the west that define the RRL (between opposing black arrows). The dashed part of the Roanoke River shows the locations of sand mounds along its natural levees. The red dot northeast of Tarboro is a small earthquake from 1895 (Reager *et al*. 1987). Black and white polygons are areas of small circular topographic depressions described in the text. PS is the location of the sandy soil shown in the photo of Figure 14. WDS and WOS are the Whiteoak and Wildcat swamps that may have once formed a continuous drainage before being interrupted by uplift along the northern side of the eastern RRL. Terrace units are from Weems *et al.* (2009) (Figure 2a). DD is the E-W-oriented drainage divide just north of the eastern RRL. Illumination azimuth is 140º. A, H, J, Lw, P, and T are towns Askewville, Hamilton, Jamesville, Lawrence, Palmyra, and Tarboro. Image location is shown in Figure 4a.

Figure 6. Examples of tar kilns in the outer Coastal Plain of eastern North Carolina northeast of Washington. Photos taken 1 March 2023. **(a)** LiDAR image showing examples of tar kilns. **(b)** Photo of typical tar kiln with an ~2-ft-high outer ring of soil surrounded by a shallow trench only a few inches deep. Note the ~1 1/2-ft-deep hole dug for the tar-collecting barrel. **(c)** Photo of an ~2-ft-high tar kiln with a flat-topped soil mound. **(d)** Photo of a ~1 1/2-ft-high tar kiln with multiple inner rings of soil. **(e)** Photo of a nearly flat tar kiln with a ~1 1/2-ft-deep depression in which the tar-collecting barrel was placed. Note the unburned portion of a pine log along the edge of the depression. Photos (b)-(e) were taken just northeast of Washington, North Carolina (Figure 1). Photos 6b and 6d are shown on the LiDAR image in diagram (a) while the other photos were taken just outside the image area.

Figure 7. Enlarged color LiDAR image that shows angular stream bends (arrows) in a Deep Creek tributary west of the Roanoke River. Stream bend A along a Deep Creek tributary forms part of the RRL. Illumination azimuth is 140º. Image location is shown in Figure 5.

Figure 8. (a) Elevation profiles 1-7 across the Roanoke River (RR) valley. Geologic units are from Weems *et al.* (2009). Unit Qal is the modern floodplain, which is entrenched below the older Holocene valley sediments labeled Qal2. **(b)** Elevation profiles 8 and 9 that cross the gentle, E-W-oriented topographic scarp along the eastern RRL. The location of terrace A is shown in Figure 4b. **(c)** Elevation profile (extracted from profile 6) across the Roanoke River and one of the sand mounds on its natural levee.

Figure 9. Sinuosities along the Roanoke River. The valley segment lengths used to generate the sinuosites were 6 km upstream from the deflection in the Roanoke River, 4 km for the valley downstream from the river deflection to near Hamilton, and 22 km downstream from Hamilton.

Figure 10. Enlarged IHS-enhanced color LiDAR image showing angular stream bends (white arrows) along Fishing Creek, the Tar River valley, and tributaries of Deep Creek west of the Roanoke River. RRL is the Roanoke River lineament. Carolina bays are labeled C. Lw and T are the towns Lawrence and Tarboro. The arrows labeled SW along the lower Tar River valley show the Tar River's area of WSW migration during late Pleistocene-Holocene time. Image location is shown in Figure 5.

Figure 11. (a) Enlarged color LiDAR image of the lower Roanoke River valley, which shows the locations of sand mounds labeled V along the Roanoke River's natural levees. Sand mound locations in Figure 12 are shown as arrows labeled 12a-12d. Image location is shown in Figure 5. **(b)** Enlarged color LiDAR image of the lower Roanoke River valley that shows examples of sand mounds. Image location is shown in diagram (a).

Figure 12. Examples of sand mounds on gray-scale LiDAR images along the Roanoke River's natural levees downstream from the RRL. Their locations are shown in Figure 11a. **(a)** Examples of sand mounds at location V3 of Figure 11a. **(b)** ENE-WSW-oriented sand mounds along the Roanoke River at location V5 of Figure 11a. **(c)** Two overlapping sand mounds with large topographic depressions at their apices near the northwest end of the sand mounds labeled V2. **(d)** Sand mound at location V10 of Figure 11a showing numerous 4- to 5-m-wide circular topographic depressions (black dots) in the terrain surrounding the mound. Note the small circular depressions aligned along the axis of the sand mound. The illumination azimuth was 115º for all images.

Figure 13. (a) Enlarged color LiDAR image north of the RRL showing examples of small circular topographic depressions (arrows). Arrow A points toward the topographic depression for which elevation profiles are shown in image (b). The image location is shown in Figure 5. Illumination direction is from the northeast. **(b)** Elevation profiles across the depression at location A in image (a).

Figure 14. Photograph of light-colored patches of sandy soil south of the lower Roanoke River valley, which we speculate could be seismically induced paleoliquefaction deposits. Photo taken 1 March 2024. See Figure 5 for photo location.

Figure 15. (a) Photograph of Burnt Coat Swamp just upstream from the right-angle bend in Marsh Swamp. **(b)** Photograph of Beech Swamp immediately downstream from the right-angle bend in Marsh Swamp. Notice the submerged, swampy nature of Beech Swamp in photo (b) compared to the dry, elevated floodplain of the Burnt Coat Swamp in photo (a). Both photos were taken 3 March 2024.

Figure 16. Conceptual model showing the spatial relationship between the interpreted Roanoke River sinistral strike-slip fault zone (RRFZ), Tarboro fault zone (TFZ), and the Tar River releasing offset (TRO) (gray pattern) between the ECFS-S and ECFS-N. The green pattern is the area between the RRFZ and TFZ. S_{Hmax} (between opposing arrows) is the orientation of the regional maximum horizontal compressive stress field (Lundstern and Zoback 2020). Red dots are small (≥MMI III) historical earthquakes between 1735 and 1983 (Reager *et al*. 1987). Yellow patterns show areas of small circular topographic depressions while the red pattern shows the area of sand mounds along the lower Roanoke River valley. The tan pattern with WSW-pointing arrows labeled SW along the lower Tar River valley shows the area of WSW river migration during late Pleistocene-Holocene time. The short-dashed pattern is the buried Graingers basin (GB). The red dashed contour shows the locations of the Albemarle embayment, Cape Fear arch (CFA), and Norfolk arch.

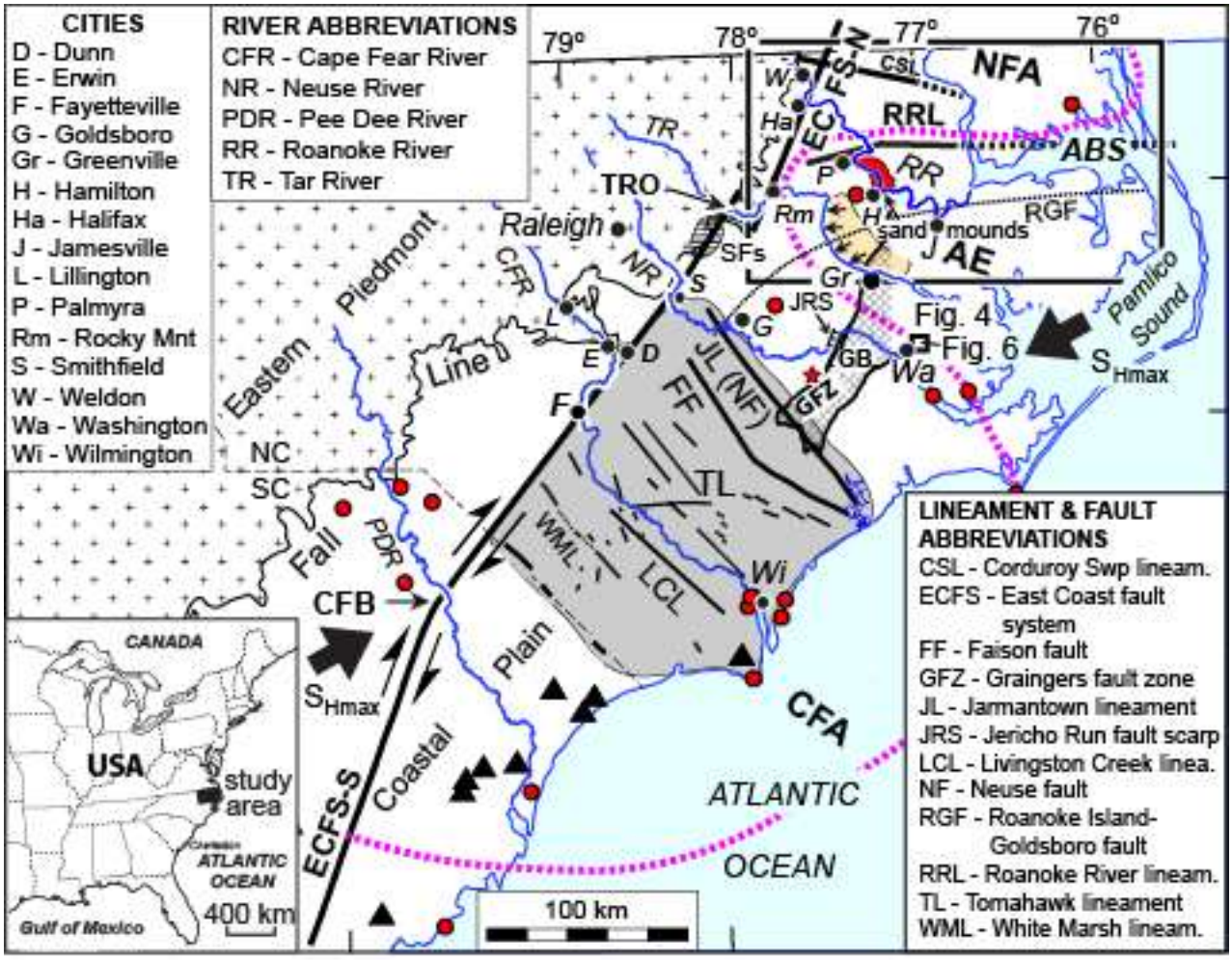
CITIES
D - Dunn
E - Erwin
F - Fayetteville
G - Goldsboro
Gr - Greenville
H - Hamilton
Ha - Halifax
J - Jamesville
L - Lillington
P - Palmyra
Rm - Rocky Mnt
S - Smithfield
W - Weldon
Wa - Washington
Wi - Wilmington
RIVER ABBREVIATIONS
CFR - Cape Fear River
NR - Neuse River
PDR - Pee Dee River
RR - Roanoke River
TR - Tar River
79°
78°
77°
76°
NFA
RRL
ABS
JAE
RGF
sand mounds
TRO
Raleigh
Piedmont
Eastern
Line
NC
SC
Fall
PDR
CFB
CFR
NR
TR
RR
SFs
JRS
Fig. 4
Fig. 6
Pamlico Sound
JL (NF)
FF
TL
WML
LCL
GFZ
GB
Coastal Plain
ECFS-S
CFA
ATLANTIC OCEAN
100 km
CANADA
USA
study area
ATLANTIC OCEAN
Gulf of Mexico
400 km
LINEAMENT & FAULT ABBREVIATIONS
CSL - Corduroy Swp lineam.
ECFS - East Coast fault system
FF - Faison fault
GFZ - Graingers fault zone
JL - Jarmantown lineament
JRS - Jericho Run fault scarp
LCL - Livingston Creek linea.
NF - Neuse fault
RGF - Roanoke Island-Goldsboro fault
RRL - Roanoke River lineam.
TL - Tomahawk lineament
WML - White Marsh lineam.

Figure 1

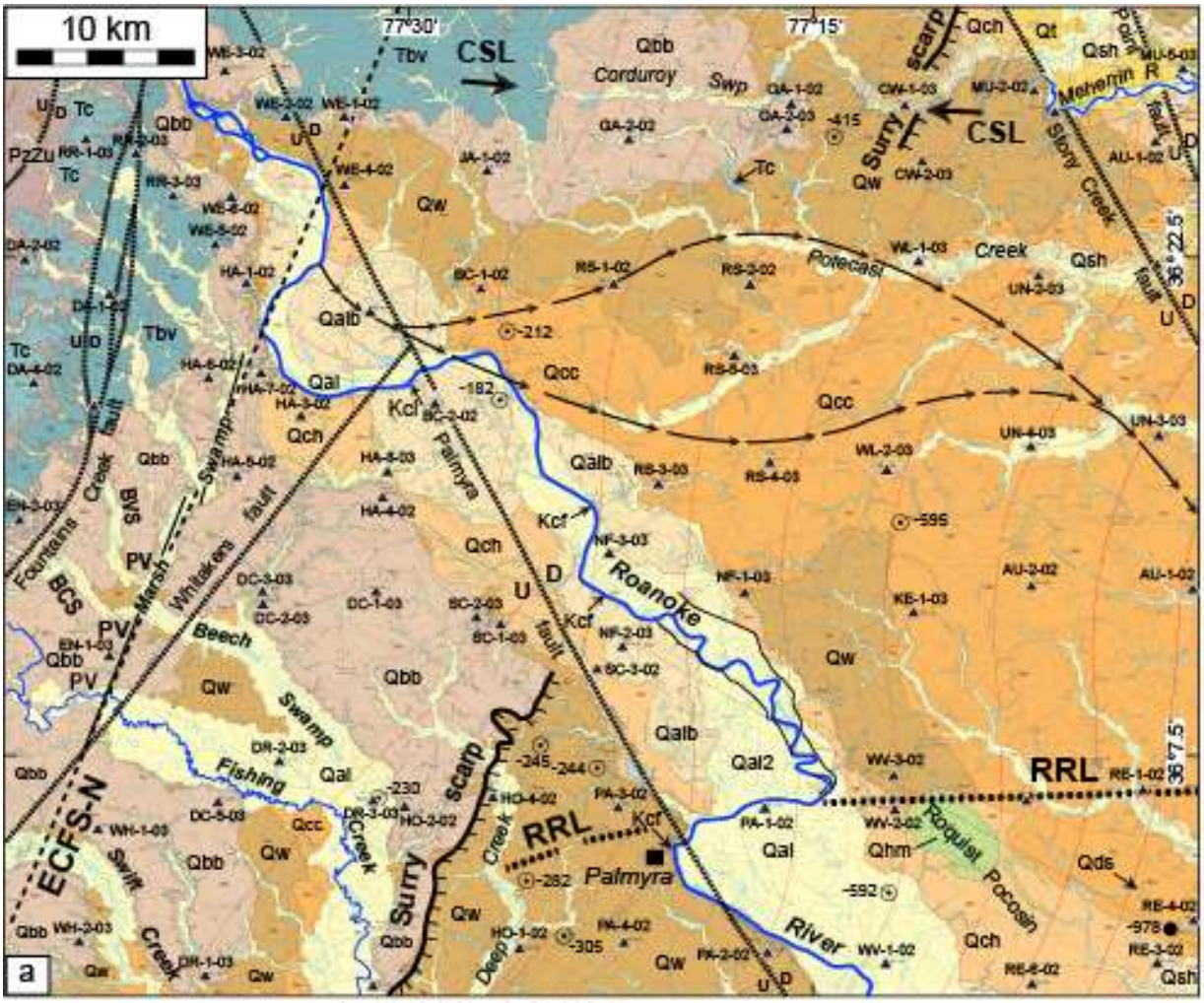

Surficial Geologic Units

Qal — Alluvium (Holocene, up to 20 ka).
Fine to coarse-grained sand containing quartz pebbles.

Qhm — Peat and Marsh (Holocene).
Organic deposits accumulating in low areas with persistently high water tables.

Qalb — Older alluvium (late Pleistocene, 20-10 ka).
Gravel, with round to subrounded quartz pebbles in a silty, medium to coarse sand matrix.

Qds — Dune sands (late Pleistocene, 80-10 ka).
Very fine to medium-grained clean sand.

Qt — Tabb Fm (late Pleistocene, 130-90 ka).
Very fine to fine-grained silty and clayey sand.

Qsh — Shirley Fm (late Pleistocene, middle Pleistocene, 250-200 ka).
Very fine to fine-grained, silty, and clayey sand.

Qcc — Chuckatuck Fm (middle Pleistocene, 450-400 ka).
Very fine to fine-grained, silty, and clayey sand.

Qchs — Chuckatuck Fm (middle Pleistocene, 450-400 ka).
Fine-grained sand.

Qcc — Charles City Fm (early Pleistocene, 1.3 Ma-730 ka).
Very fine to fine-grained silty and clayey stiff sand.

Qw — Windsor Fm (early Pleistocene, 1.3 Ma-730 ka).
Very fine to fine-grained, silty and clayey stiff sand.

Bacons Cattle Formation

Qbb — Bahramsville unit (early Pleistocene, 1.7-1.6 Ma).
Very fine to fine-grained silty and clayey stiff sand.

Tbv — Varina grove unit (Upper Pliocene, ~2 Ma).
Very fine to fine-grained, silty and clayey stiff sand.

Tc — Chowan River Fm (Upper Pliocene, ~2.5 Ma).
Very fine to fine-grained, silty and clayey, stiff sand.

Yorktown Formation

Tyrm — Rushmere and Morgarts Beach Members, undivided (middle Pliocene, 3.5-3.0 Ma).
Clayey silt and very fine-grained sandy to silty and clayey very fine-grained sand.

Kcf — Cape Fear Fm (Upper Cretaceous, ~87 Ma).
Clayey silt.

Kcl — Clubhouse Fm (Upper Cretaceous, ~95 Ma).
Very fine to medium-grained, clayey and silty sand.

PzZu — Roanoke Rapids terrane (early Paleozoic and Neoproterozoic, 600-500 Ma).
Upper greenschist to lower amphibolite facies rocks.

Paleochannels of the Roanoke River.
Arrows indicate flow direction.
RRL - Roanoke River lineament

DC-1-03 U.S. Geological Survey auger hole.
●-978 U.S. Geological Survey corehole-Basement elevation in feet.
⊙-282 Other basement well data-Basement elevation in feet.
Joints along Marsh Swamp

Figure 2

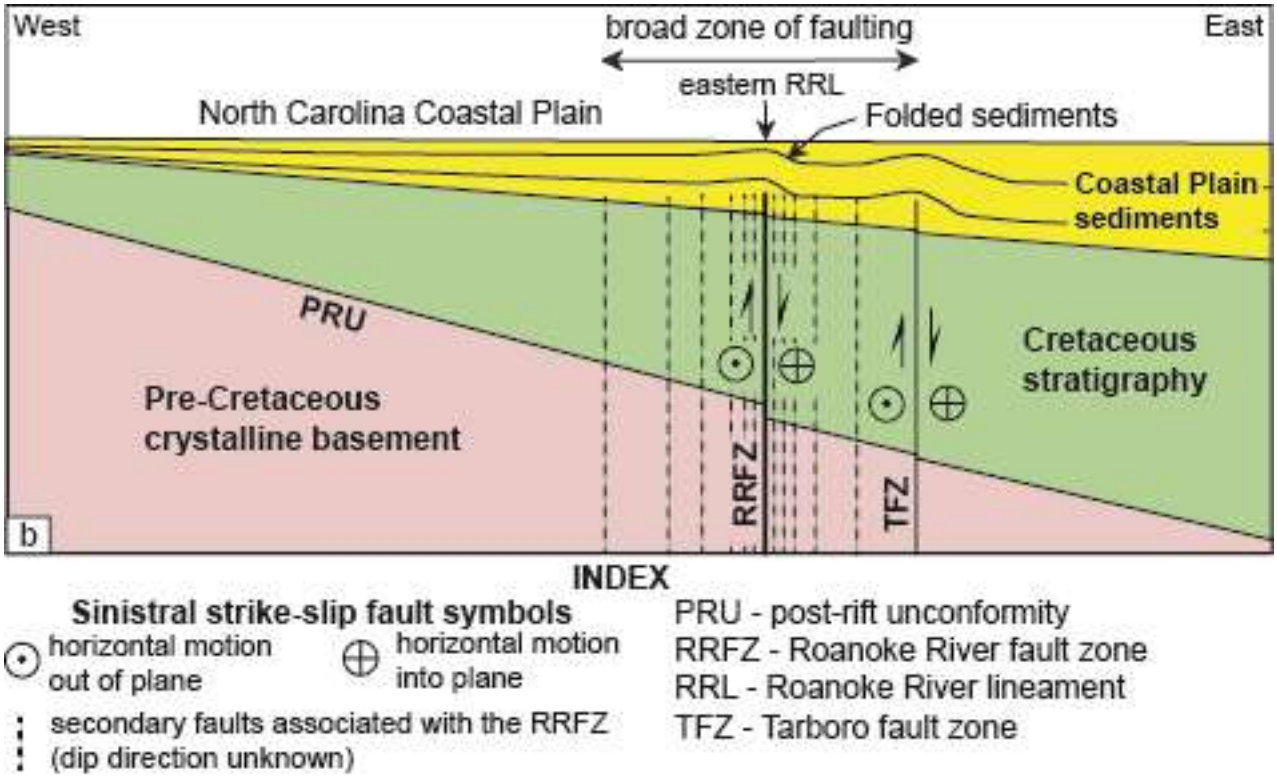
West
broad zone of faulting
East
eastern RRL
North Carolina Coastal Plain
Folded sediments
Coastal Plain sediments
PRU
Cretaceous stratigraphy
Pre-Cretaceous crystalline basement
RRFZ
TFZ
b
INDEX
Sinistral strike-slip fault symbols
horizontal motion out of plane
horizontal motion into plane
secondary faults associated with the RRFZ (dip direction unknown)
PRU - post-rift unconformity
RRFZ - Roanoke River fault zone
RRL - Roanoke River lineament
TFZ - Tarboro fault zone

Figure 2b

Figure 3

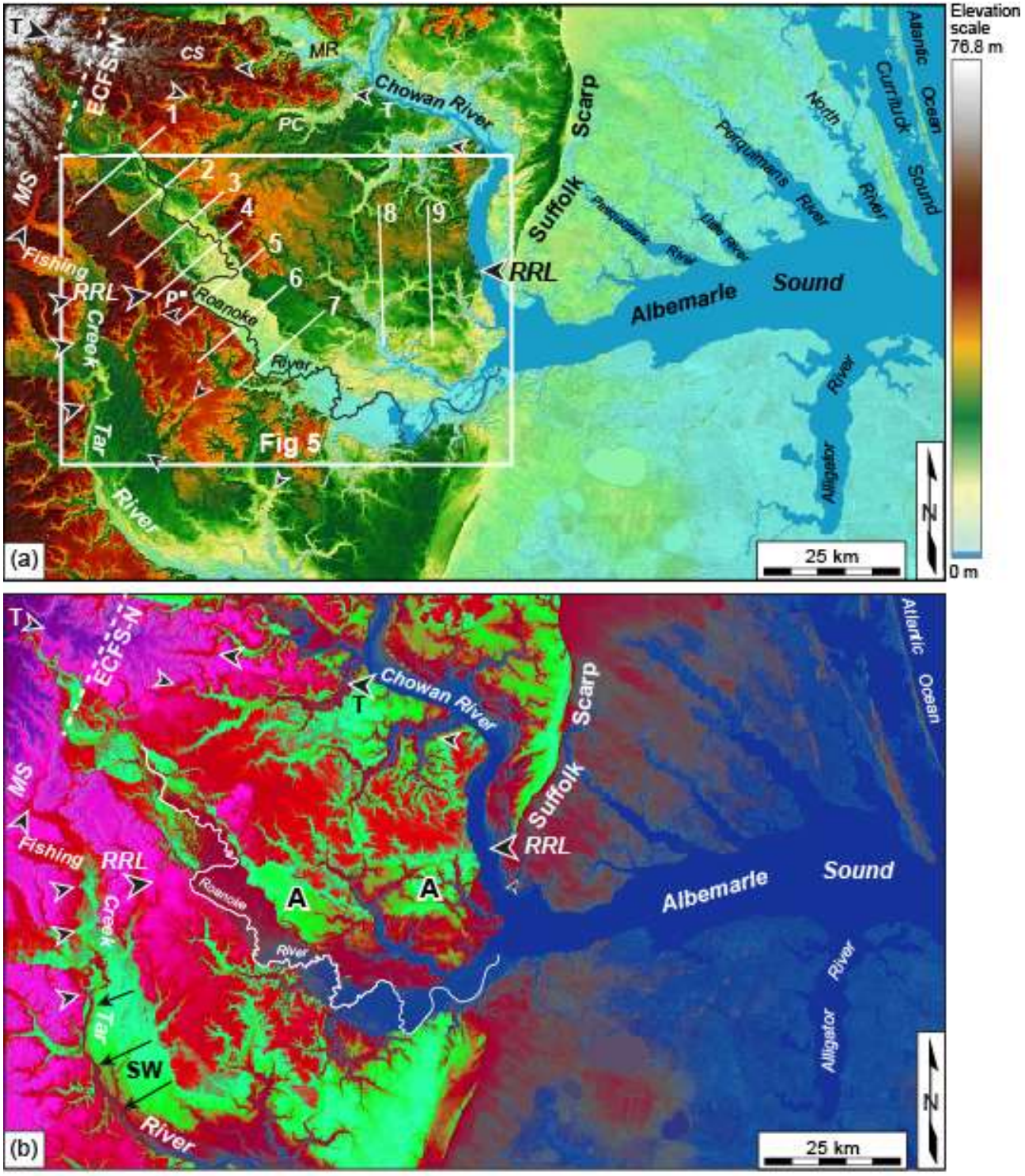
(a)
ECFS-N
CS
MR
PC
Chowan River
Scarp
Suffolk
RRL
Albemarle Sound
Atlantic Ocean
Currituck Sound
North River
Pasquotank River
Perquimans River
Little River
MS
Fishing
RRL
Roanoke River
Creek
Tar River
Fig 5
Alligator River
25 km
N
Elevation scale
76.8 m
0 m
(b)
ECFS-N
Chowan River
Scarp
Suffolk
RRL
Albemarle Sound
Atlantic Ocean
MS
Fishing
RRL
Roanoke River
Creek
A
A
Tar River
SW
Alligator River
25 km
N

Figure 4

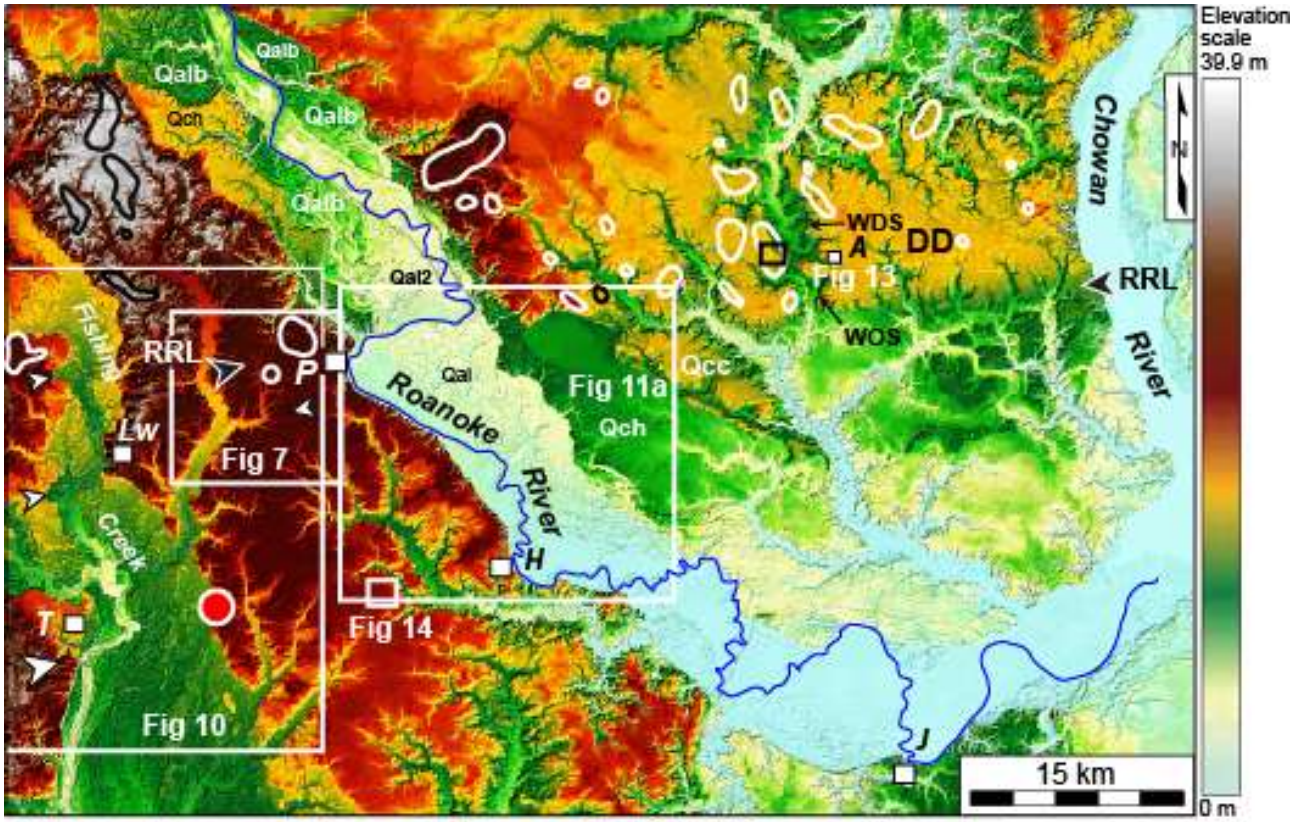
Elevation scale
39.9 m
0 m
Qalb
Qch
Qal2
Qal
Qcc
Roanoke River
Chowan River
Fishing Creek
RRL
WDS
A
DD
Fig 13
WOS
Fig 11a
Fig 7
Fig 14
Fig 10
Lw
P
H
T
J
15 km
N

Figure 5

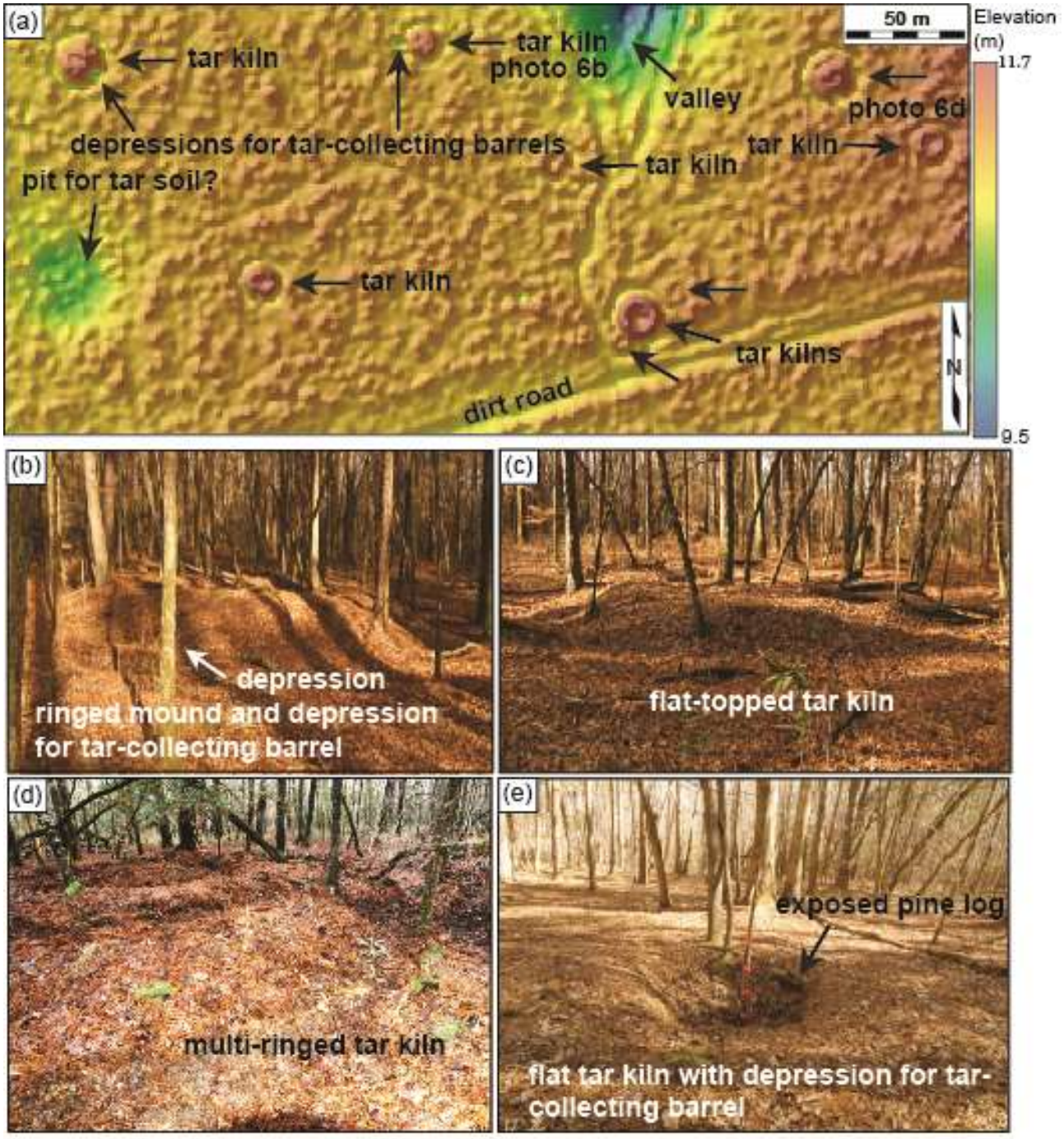
(a)
50 m
Elevation (m)
11.7
9.5
tar kiln
tar kiln photo 6b
valley
photo 6d
depressions for tar-collecting barrels
tar kiln
tar kiln
pit for tar soil?
tar kiln
tar kilns
dirt road
N
(b)
depression
ringed mound and depression for tar-collecting barrel
(c)
flat-topped tar kiln
(d)
multi-ringed tar kiln
(e)
exposed pine log
flat tar kiln with depression for tar-collecting barrel

Figure 6

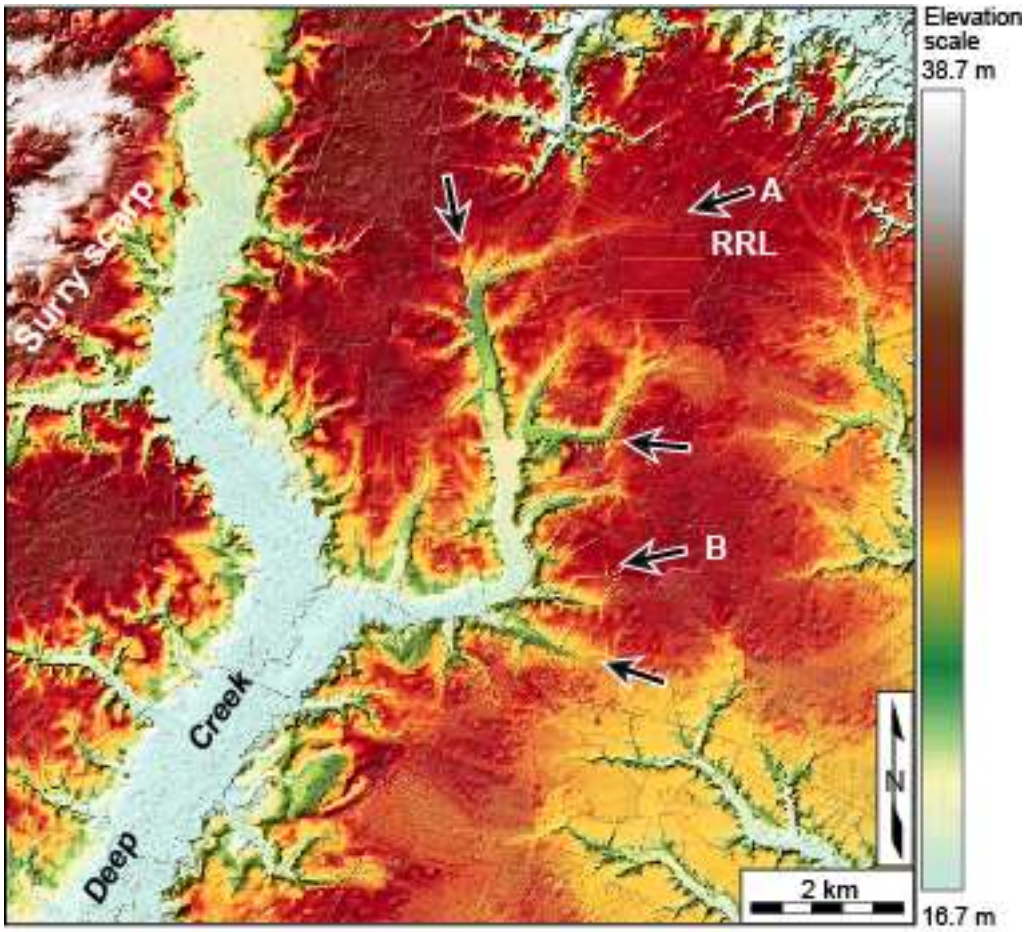
Elevation scale
38.7 m
16.7 m
Surry scarp
A
RRL
B
Deep Creek
N
2 km

Figure 7

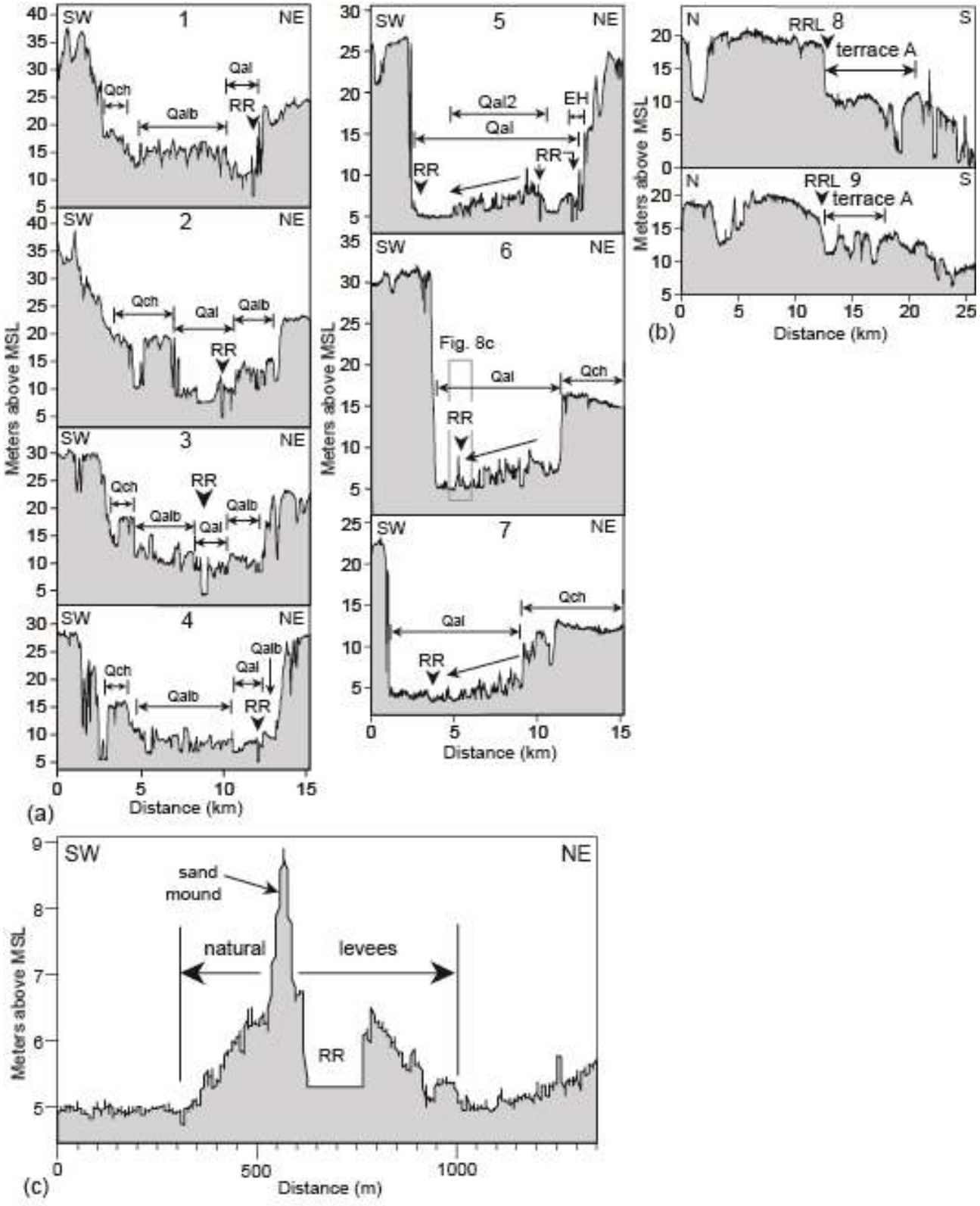
SW
NE
1
2
3
4
5
6
7
Qch
Qal
Qalb
Qal2
EH
RR
Fig. 8c
Meters above MSL
Distance (km)
(a)
N
S
RRL 8
RRL 9
terrace A
(b)
sand mound
natural
levees
Distance (m)
(c)

Figure 8

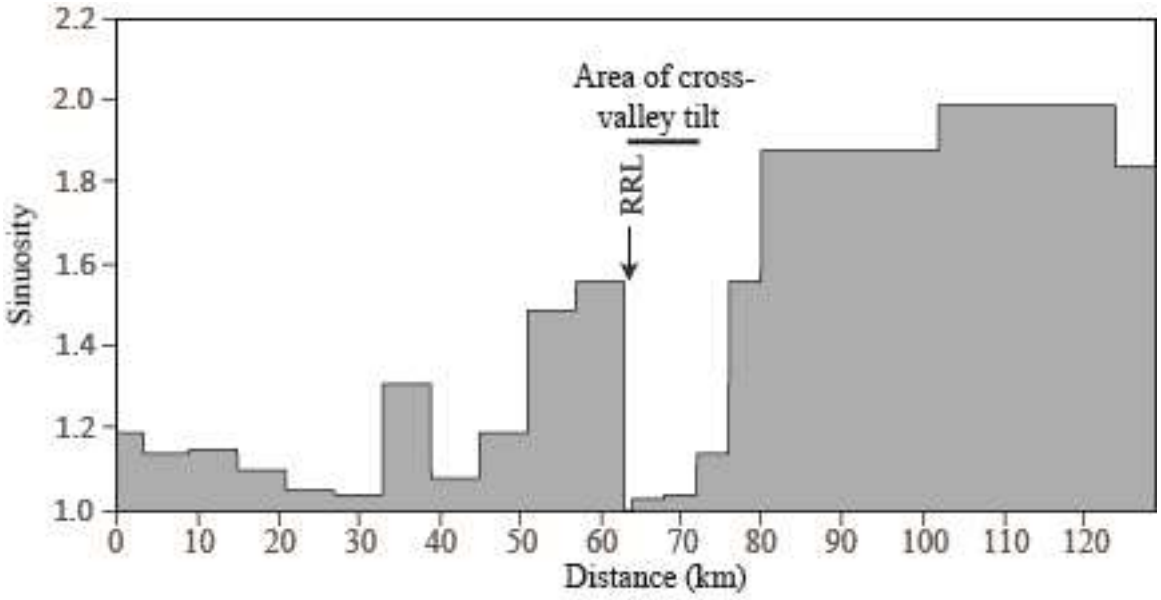
Area of cross-valley tilt
RRL
Sinuosity
2.2
2.0
1.8
1.6
1.4
1.2
1.0
0
10
20
30
40
50
60
70
80
90
100
110
120
Distance (km)

Figure 9

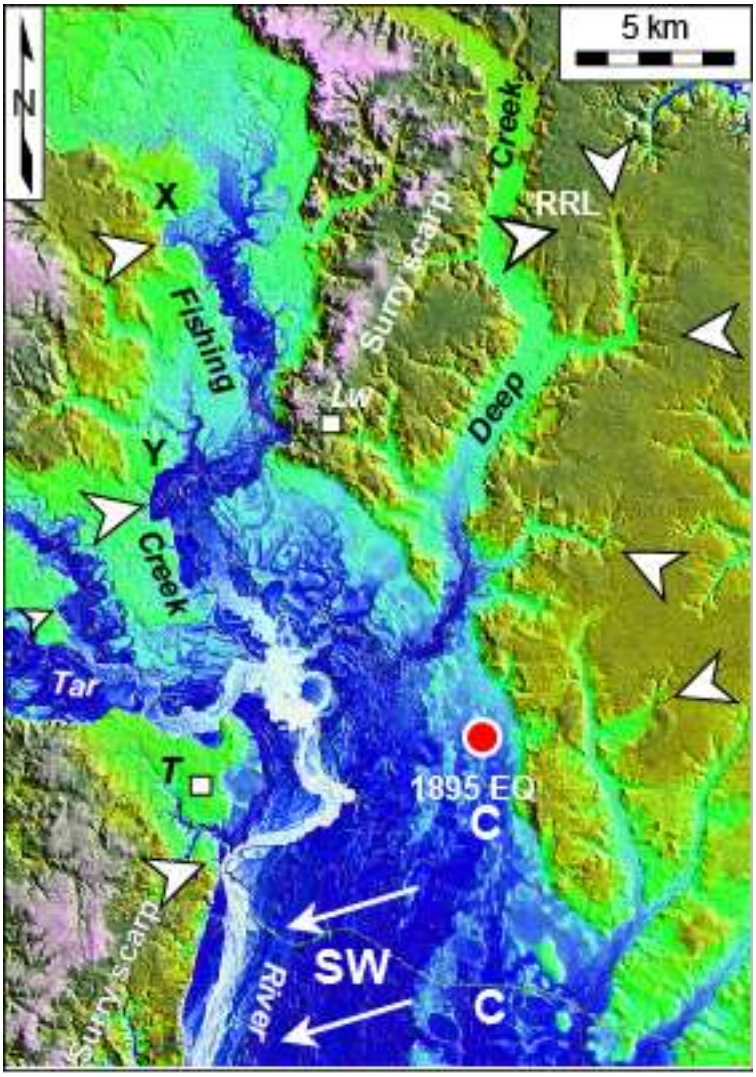
5 km
N
X
Fishing
Creek
Y
Creek
Tar
T
Lw
Surv scarp
Creek
RRL
Deep
1895 EQ
C
SW
River
C
Surv scarp

Figure 10

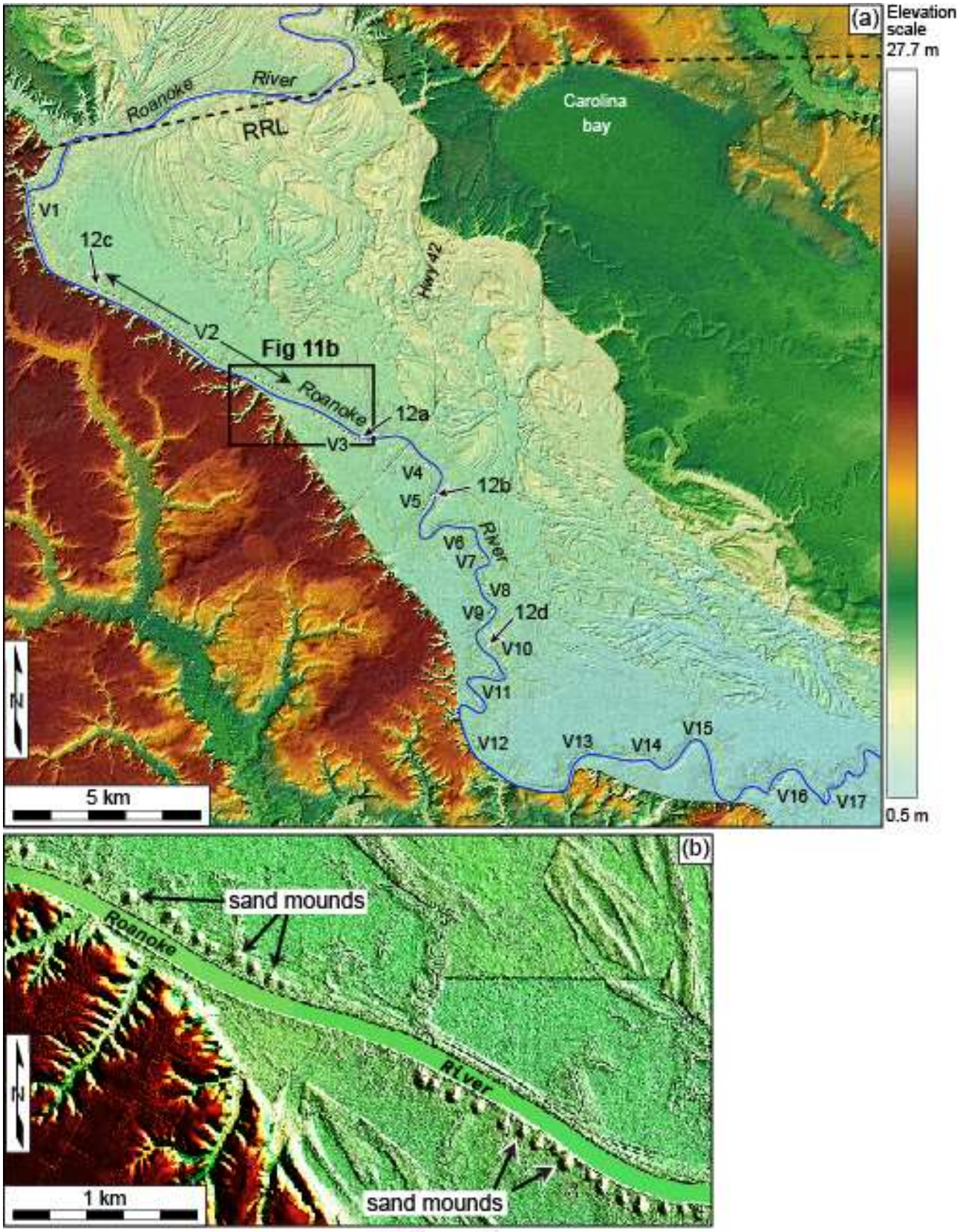
(a)
Elevation scale
27.7 m
0.5 m
Roanoke River
RRL
Carolina bay
V1
12c
Hwy 42
V2
Fig 11b
Roanoke
12a
V3
V4
V5
12b
River
V6
V7
V8
V9
12d
V10
V11
V12
V13
V14
V15
V16
V17
N
5 km
(b)
sand mounds
Roanoke
River
N
1 km
sand mounds

Figure 11

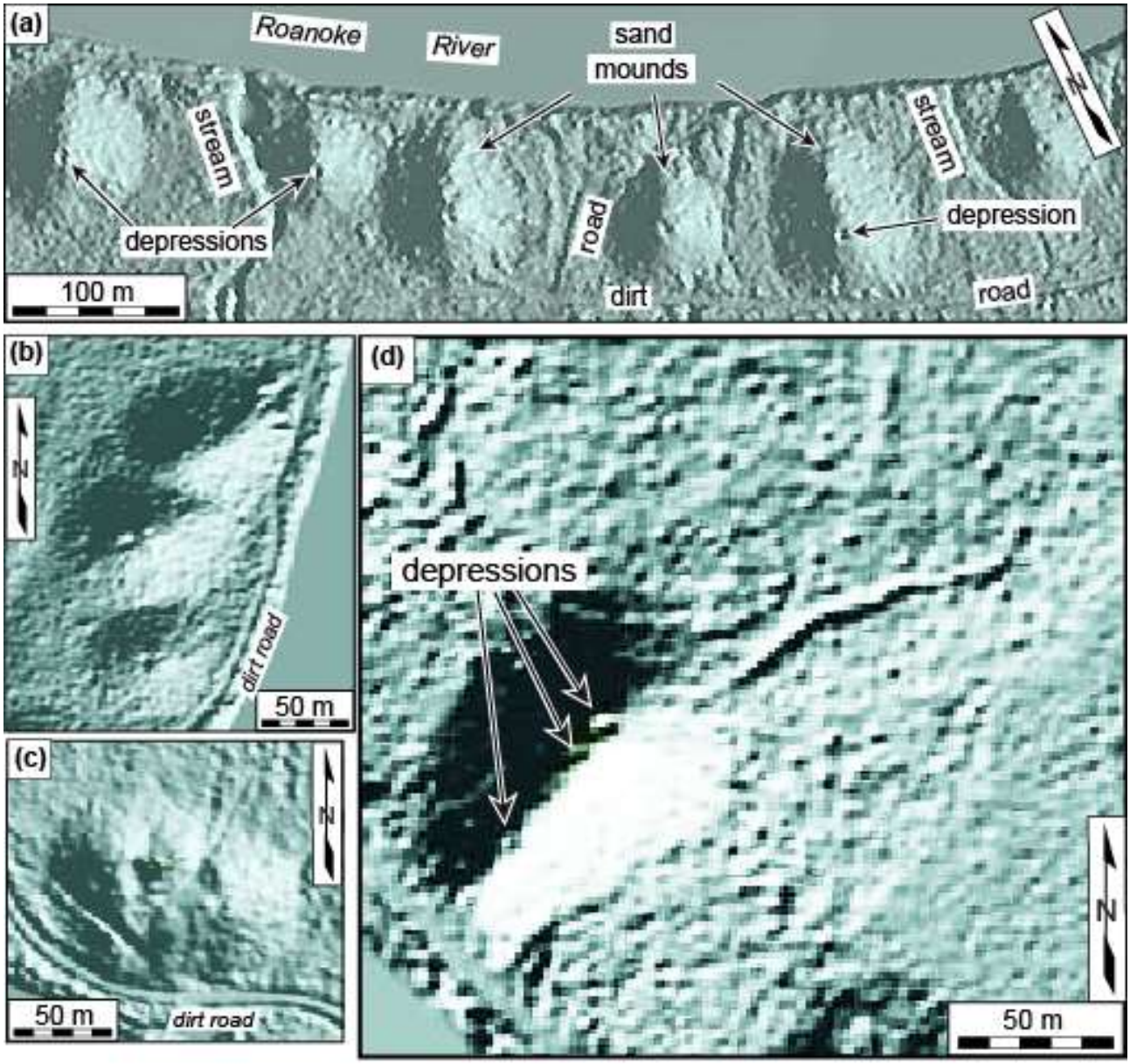
(a)
Roanoke
River
sand
mounds
stream
stream
depressions
road
depression
100 m
dirt
road
(b)
N
dirt road
50 m
(c)
N
50 m
dirt road
(d)
depressions
N
50 m

Figure 12

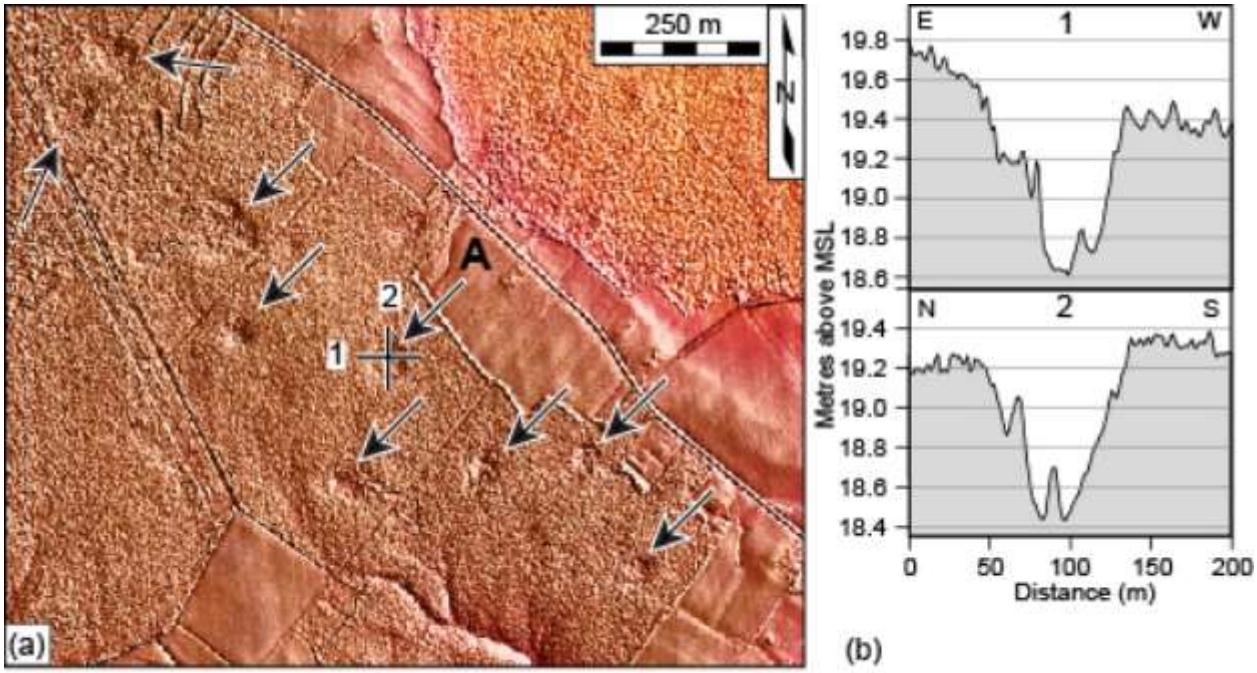
250 m
N
A
2
1
(a)
E
1
W
19.8
19.6
19.4
19.2
19.0
18.8
18.6
N
2
S
19.4
19.2
19.0
18.8
18.6
18.4
Metres above MSL
0
50
100
150
200
Distance (m)
(b)

Figure 13

Figure 14

Figure 15

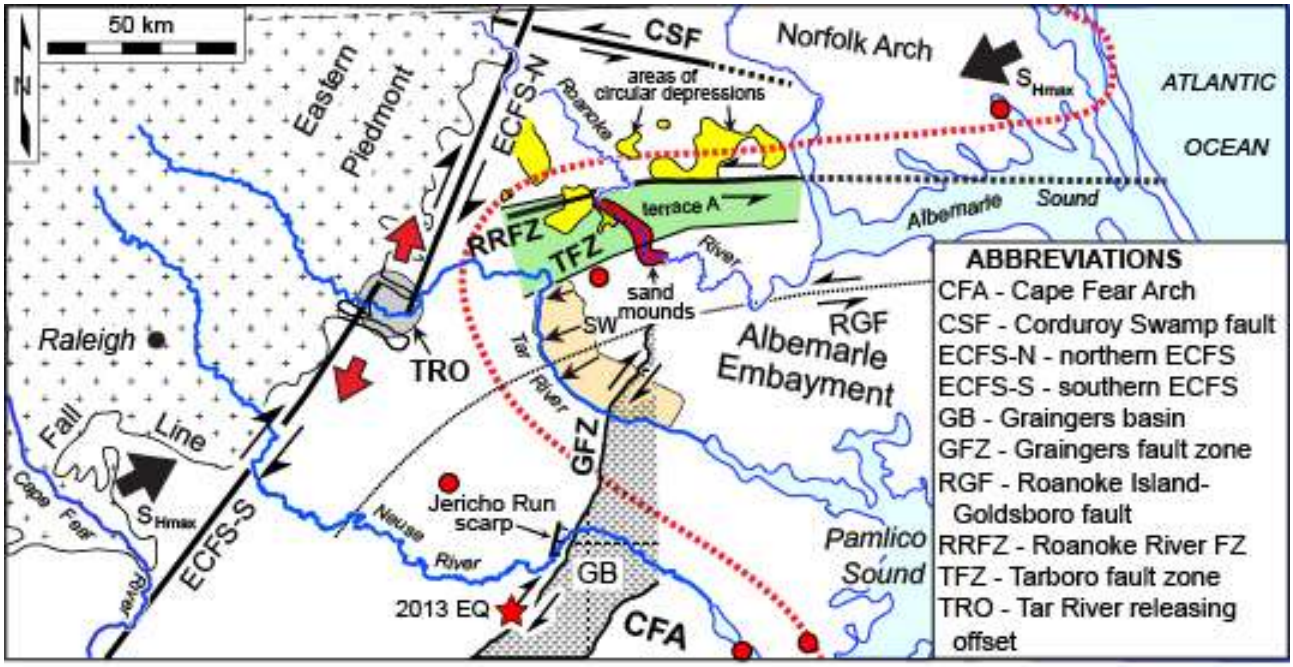
50 km
N
CSF
Norfolk Arch
S_{Hmax}
ATLANTIC
OCEAN
Eastern
Piedmont
ECFS-N
areas of
circular depressions
Roanoke
terrace A
Albemarle
Sound
RRFZ
TFZ
River
sand
mounds
SW
RGF
Albemarle
Embayment
Raleigh
TRO
Tar
River
GFZ
Fall
Line
Cape
Fear
River
S_{Hmax}
ECFS-S
Jericho Run
scarp
Neuse
River
Pamlico
Sound
GB
2013 EQ
CFA
ABBREVIATIONS
CFA - Cape Fear Arch
CSF - Corduroy Swamp fault
ECFS-N - northern ECFS
ECFS-S - southern ECFS
GB - Graingers basin
GFZ - Graingers fault zone
RGF - Roanoke Island-
Goldsboro fault
RRFZ - Roanoke River FZ
TFZ - Tarboro fault zone
TRO - Tar River releasing
offset

Figure 16